AN EVALUATION OF A SMALL HYDROCLONE USING ELECTRICAL ANALOG TECHNIQUES

By

JOEL STERLING GILBERT

Bachelor of Science

University of Oklahoma

Norman, Oklahoma

1958

Submitted to the Faculty of the Graduate School of
the Oklahoma State University
in partial fulfillment of the requirements
for the degree of
MASTER OF SCIENCE
August, 1960

AN EVALUATION OF A SMALL HYDROCLONE

USING ELECTRICAL ANALOG TECHNIQUES

Thesis Approved:

R. E. Chapel
Thesis Adviser

J. H. Boggs

Dean of the Graduate School

PREFACE

No analytical means for evaluating a hydroclone in terms of separation of solids from liquids is presently available. The need for an adequate solution to this problem in the field of liquid-solid separation has prompted this investigation.

I sincerely wish to thank Dr. J. H. Boggs for the Research Assistantship which I have held while attending Oklahoma State University. A generous thanks goes to Professor A. G. Comer and Professor R. E. Chapel for their continued advice and encouragement throughout the course of this study as my advisers. Without the help of Professor George Lucky, Professor Don Haworth, and Dr. John Wiebelt, the application of the analytical expression to the Donner Electrical Analog Computer would have been extremely difficult. The laboratory assistance of Mr. John McCandless was very valuable in this investigation. I wish to say thanks to Sonya Giddens for her efficient and capable services as my typist. To my wife, Evelyn, go my thanks for the patience and understanding she had in order that I might receive my education.

TABLE OF CONTENTS

LIST OF TABLES

LIST OF FIGURES

CHAPTER I

INTRODUCTION

Although the liquid-solid hydroclone is a relatively recent innovation in the field of liquid-solid separation, it is similar in construction and operation to the older and more familiar gas cyclone dust collector.

A brief description of the flow pattern of the liquid and the reaction of the solids will acquaint the reader with the operating principles of a hydroclone. The hydroclone consists of a cylindrical section mounted above a truncated cone. The feed nozzle enters the cylindrical ring tangentially with the underflow nozzle, which permits discharge of the concentrated solids, located at the apex of the cone. The overflow nozzle is centered in the cylindrical section of the hydroclone. The flow path is simply a double vortex pattern; one vortex moves downward along the hydroclone wall and leaves through the underflow nozzle while the other vortex moves upward in the center of the hydroclone and leaves through the overflow nozzle. The liquid from which the solids have been removed leaves through the overflow nozzle. If the solid particles are of sufficient size and gravity they are ejected outward to the walls and discharge spirally to the underflow. Most of the liquid with the uneliminated fine solids moves radially inward along the path of the outer spiral to a second inner spiral at the cyclone core to pass out the overflow. The most critical

fluid movement because of its small radius and high tangential velocity is the inner spiral.

Using an underflow pot rather than having a separate discharge line from the hydroclone has been found to be satisfactory with a limited amount of underflow. An underflow pot is a reservoir in which the solids from the underflow can settle out.

A hydroclone with an underflow pot is a possible answer to the problem of removing contaminants from fluid. Under Contract No. AF 34(601)-5470 with Oklahoma City Air Materiel Area, Tinker Air Force Base, Oklahoma, the Mechanical Engineering School of Oklahoma State University is currently conducting tests to determine the effectiveness of hydroclones. Demands by the aircraft and missile industry for more precise and reliable hydraulic system performance require that hydraulic fluid contamination be controlled. Contaminants are composed of not only products of oxidation, but also intrinsic contaminants, such as water, metallic solids, dirt and other extraneous materials. In this study glass beads of specific size ranges are used as artificial contaminants. Any contaminant which is equal to or greater than the smallest clearance in a hydraulic system can cause excessive wear and malfunctioning.

Many current military specifications for filters require that 98% of the particles of a certain size or larger be eliminated from the hydraulic fluid. This type of specification has limited meaning because the 2% unaccounted for can cause considerable damage. On this basis, if it can be stated that all contaminants greater than a certain value are removed from the hydraulic fluid by a hydroclone, then a designer will know what the smallest clearance in a servo valve or other component could be.

CHAPTER II

PREVIOUS INVESTIGATIONS ON HYDROCLONES

Only in the past ten years has real progress been made in understanding the phenomena occurring in the hydraulic cyclone, more commonly called the hydroclone. This summary consists of only the most pertinent studies made by scientists and engineers in the field of liquid-solid separation.

Dahlstrom (1) established two empirical equations of importance. The first one deals with the factors of pressure drop and capacity. It is as follows:

$$\frac{Q}{\sqrt{\Delta P}} = K(d_o\, d_r)^{0.9} \quad . \tag{2-1}$$

The constant, K, is affected most by such parameters as the separation between overflow and the conical section, cone included angle, and the type of underflow discharge.

The second empirical equation involves solid elimination efficiency. In operation, the fraction of solids eliminated from the feed to a liquid-solid cyclone is probably more important than the accompanying energy loss. The determination of the 50%-point is the most common method of measuring extraction efficiency. This represents the particle which reports 50% by weight to the overflow and 50% by weight to the underflow. The 50%-point also provides a limit of extraction efficiency because very little material of similar specific gravity, but larger in size, will be found in the overflow stream, and by the same reasoning only a relatively

small amount of particles finer than the 50% dimension will report to the underflow. This second equation is as follows:

$$D_{50} = \frac{K_1 (d_o\, d_i)^{0.68}}{(Q)^{0.53}} \left[\frac{1.73}{\rho_s - \rho_l}\right]^{0.5} . \qquad (2\text{-}2)$$

Dahlstrom (1) determined that Stokes' Law could be used to predict the effect of solid specific gravity upon the 50%-point. Experimental work confirmed the solid elimination efficiency equation.

Criner (2) brought forth an explanation of the movement of liquids and solids in the hydroclone. After a discussion of the force fields in the fluid a calculation of velocities in a cylindrical vortex of two dimensions was developed. This development takes into account the effect of "turbulent viscosity" and the radial flow. Taking into account the radial flow in each normal section, an approximation of values of velocities parallel to the axis was established. The distribution of the tangential velocities was assumed to be hyperbolic.

One of the significant contributions of Criner (2) was the locating of a plane in the hydroclone perpendicular to the axis of the hydroclone which is a measure of the amount of underflow. All fluid passing this "plane of no return" leaves the hydroclone at the underflow nozzle. The underflow, Q_u, divided by the total flow, Q, times L, the distance between the bottom of the overflow nozzle and the underflow opening, is equal to Z. That is to say,

$$Z = L \cdot \frac{Q_u}{Q} \quad , \qquad (2\text{-}3)$$

where Z is the distance separating the above mentioned plane and the

underflow nozzle. The flow ratio, $\frac{Q_u}{Q}$, is described along with the three characteristic flow patterns in a hydroclone by Criner (2).

The trajectories of solid particles in suspension were deduced from fluid velocities and the relative velocity of particles with regard to the fluid. The solids must move through the hydroclone assuming the velocity of the fluid at every point except where motion relative to the fluid is induced by forces due to the acceleration of the solids. This statement can be true only for particles of zero size and is only approximate for particles of finite size. Criner (2) took into account the influence of volumetric concentration of the particles. Observation of experimental facts furnished the parameters of calculation and supported the conclusions drawn from this theoretical analysis.

In the study of flow in a hydroclone Driessen (3) first developed appropriate equations taking into account the influence of turbulence, and second, verified the equation from experimental data.

The equations of Navier-Stokes in polar coordinates were applied to the hydroclone with the hypothesis that the flow in a hydroclone can be compared to a two-dimensional vortex in an incompressible viscous medium. After making simplifying assumptions the following equation results:

$$\frac{A^2}{(2\pi)^2 r^3} + \frac{V^2}{r} = \frac{1}{\rho} \frac{dP}{dr} \quad , \qquad (2\text{-}4)$$

where

$$A^* = -V_r \, r \, 2\pi .$$

---

*For a centripetal or negative flow V_r will be negative and "A" must be considered as positive. "A" is the flow constant of fluid running through the coaxial cylinders for a unit height.

By letting $n = -\frac{A}{2\pi\beta} + 1$, the above equation reduces after integrating to

$$V = \left[\frac{C}{n+1}\right] r^n + \frac{C_1}{r} \quad . \tag{2-5}$$

This equation is the fundamental solution of the differential equation of two-dimensional flow of a vortex in viscous fluid.

The constants C and C_1 of the equation for tangential velocity can be calculated, if the boundary conditions are given; for example a known tangential exterior velocity V_2 at radius r_2 and an interior velocity V_1 at radius r_1.

One type of flow that does occur in practice can be represented by letting $n = -1$ or $\beta = \frac{A}{4\pi}$. Using what is referred to as the "Logarithmic solution," the tangential velocity takes the form

$$V = \frac{V_2 r_2}{r} \left[\frac{1 + \ln\frac{r}{r_1}}{1 + \ln\frac{r_2}{r_1}}\right] \quad . \tag{2-6}$$

Driessen (3) proved the mathematical relations he developed by measuring the static pressures which prevail in the hydroclone at different radii. From the various pressures the distribution of the tangential component of velocity can be deduced with the help of the equation (2-4).

In this particular case, the equation for tangential velocity coincides with the experimental measurements.

The coefficient of turbulent viscosity, β, is 468 times larger than the coefficient of actual kinematic viscosity, ν, of air at 20°C, as it was measured during the course of his experiment.

The discussion presented by Moder (4) was slanted for application to

the chemical processing industry. This experimental investigation determined to be the separation power, optimum design, and energy requirement of a single hydroclone and a multiple hydroclone arrangement. The conditions proposed by Moder (4) were for rapid separation of solid materials of similar specific gravities. This process utilizes a liquid which will float the less dense material and sink the more dense material without affecting the solids being separated during short contact periods. A mixture of the liquid and the solids to be separated would be fed into one or more hydroclones in series. The sink and float material concentrated in the underflow and overflow streams respectively.

Kelsall (5) in his excellent fundamental study used a microscope with stationary and rotating objectives to measure particle velocities and directions within the hydroclone. He observed fine aluminum particles within a transparent hydroclone.

Three series of experiments were carried out at indicated feed pressures of 10, 20, 30 and 40 pounds force per square inch. The first series involved negligible underflow discharge, the second no overflow and in the third series both underflow and overflow were obtained.

Vertical and radial velocity components are important in the fields of fluid mechanics of the hydroclone. The former component indicates the magnitude of the two spirals and determines the volume distribution between overflow and underflow; the latter is the fluid current against which the particle must settle in order to be removed in the underflow. In a 3-inch hydroclone the particle velocity was found to attain at least 95% of the fluid velocity at any radius for the fine solids employed.

Kelsall (5) found that the vertical velocity profile was independent

of pressure drop or flow rate. Therefore a typical plot of the vertical velocity profile with suitable scale change would hold for any pressure drop. Furthermore, feed volume fractions to the underflow as high as 0.60 did not affect the profile contours. The zero vertical velocity point, which defines the division between the two spiral patterns, is slightly inclined off the vertical; however, uniformity in vertical velocity profile below the vortex finder is still relatively good.

Radial velocity profiles were found also to be independent of pressure drop and flow rate. Below the vortex finder, radial velocity decreases as the radius decreases. Above the vortex finder there is an outward component to supply the recirculation occurring in this region. Immediately at the vortex finder level there is evidence of outward radial velocities, which Kelsall (5) believes accounts for a slight lowering in separation efficiency. It should be pointed out, however, that his vortex finder extended into the conical section, which is known to decrease separation power and classification sharpness.

Kelsall (5) in his investigation indicated excellent agreement with Criner and Driessen (2, 3) by using a 20° included angle, 3-inch diameter hydroclone and employing the hypothesis of the equilibrium radius proposed earlier by them. This is the radius at which the resultant radial settling velocity of a particle due to centrifugal force exactly equals the inward radial velocity of the liquid. As Stokes' Law is known to apply,

$$V_r = \frac{V^2 D^2 (\rho_s - \rho)}{18 r_e \mu} \quad . \qquad (2\text{-}7)$$

As he observed both radial and tangential velocities, it was possible to calculate values of the equilibrium radii for the solid used in his

investigation. Applying this law to the settling process, equilibrium envelopes were derived for particles of several sizes and a measure of the particle separation efficency was obtained. Relationships were derived between total volume flow rate and the tangential velocity at any point, and total volume flow rate and separation efficiency. The negligible effect on separation efficiency of a change in percentage of the total flow discharged to underflow was demonstrated.

Two important "secondary" flows were noted, one involving a recirculation of liquid and solid particles at levels above the bottom of the vortex finder and the other a short circuit flow with low particle separation efficiency down the outside wall of the vortex finder to the overflow.

By a technique involving injection of closely sized batches of "Perspex" spheres into the feed of a 3-inch hydroclone, Kelsall (6) investigated the effect of several variables on solid elimination efficiency.

A ¼-inch feed diameter resulted in maximum efficiencies in this hydroclone for a wide range of conditions. It was considered impossible to derive simple power relations to describe the effect on particle elimination efficiency of a change in feed diameter, overflow diameter, or flow rate.

The importance of turbulent mixing in the feed section due to shock effects and of the short circuit flow down the outside wall of the vortex finder was demonstrated by Kelsall (6).

In Dahlstrom's (7) more recent discussion of hydroclones some new ideas are brought forth along with a summation of proven theory.

The outer spiral, one of the two principal flow patterns existing

within a hydroclone, travels toward the apex while the inner spiral rotates in the same manner toward the vortex finder. The outer radius of the inner spiral and the inner radius of the outer spiral appears to increase until it is slightly larger than the vortex finder radius at the plane of entrance to this overflow discharge. Because the direction of the inner spiral is toward the vortex finder, an air core is present in the cyclone if both overflow and underflow discharges are at atmospheric pressure. Correct application of back pressure to the underflow, however, will eliminate the air core without loss of separation efficiency.

Two methods of designating the classification point or separating power of the hydroclone has been presented in literature up to now. The first employs the 50% point, which is the particles' size in microns that reports 50% by weight, to the underflow and the overflow stream. The second is called the mesh of separation---the diameter in microns at which 1½% by weight of the overflow solids would be coarser. The latter therefore represents approximately the top size that would be found in the overflow stream.

Even though the hydroclone diameter has been proved to be relatively unimportant in affecting classification size and energy requirements, according to Dahlstrom (7) certain design practices should be followed in this regard. To obtain the sharpest classification at the minimum particle size for a certain pair of inlet and overflow diameters, the latter should cover a definite portion of the hydroclone diameter. Generally speaking, twice the feed diameter plus the overflow diameter divided by the hydroclone diameter should range from 0.35 to 0.70.

Hydroclones with smaller values than these will encounter excessive fluid friction and hydroclones with larger values will exhibit short circuiting to the overflow.

Haas (8) developed the hydroclone to remove 1-micron solid particles from an aqueous solution to provide a simple, durable liquid-solid separation apparatus. This apparatus removed precipitated fission and corrosion products from uranyl sulfate solutions employed in aqueous homogeneous reactors. These units ranged from 0.16 inches to 0.50 inches in diameter.

The optimum dimension ratios were determined experimentally by Haas (8) on the basis of the 50%-point. This was done for two types of underflow. First the ordinary underflow as discussed in all previous literature and second, the underflow pot which traps and holds contaminates in a closed reservoir connected to the underflow nozzle. Haas (8) is the only author to suggest the use of an underflow pot. The concentrated heavy phase flows through the underflow port after passing along the hydroclone walls. An equal volume of pot solution returns through the center region of the underflow port. Settling out in the underflow pot could increase the effectiveness of a hydroclone operated in this way. However, contaminants collected by a hydroclone might not settle out because of their small particle size and the presence of thermal convection currents. The ratio of the volume flows of the induced underflow and the hydroclone feed is determined by the geometry of the hydroclone. Induced underflows of 0 to 4% by volume of the feed flow were possible without large changes in hydroclone efficiency.

Matschke (9) pointed out the following established design criteria

for larger hydroclones. This design information will provide an engineer with necessary data to build a functional hydroclone.

A brief summary of these geometric guides is as follows:

1. The included angle should be as small as possible and still provide necessary internal flow patterns.

2. The bottom of the vortex finder should be six inches or one hydroclone diameter, whichever is less, from the transition point between the conical and cylindrical sections.

3. To allow the entering fluid to descend at least one inlet nozzle diameter in the first revolution the inlet nozzle needs to make a small angle (about 5°) with the top of the hydroclone.

4. The vortex finder should extend just below the bottom of the feed inlet to the hydroclone.

5. From the following equations the inlet and overflow dimensions are determined with respect to the hydroclone diameter.

$$\frac{2d_i + d_o}{d_h} = 0.35 \text{ to } 0.70 \ , \tag{2-8}$$

and

$$\frac{d_o}{d_i} = 1.0 \text{ to } 1.6 \ . \tag{2-9}$$

6. To minimize secondary flows which result in an overall decrease in efficiency, the distance between the top of the inlet and the hydroclone top should be kept at a minimum.

Matschke (9) found that the equation

$$\frac{Q}{\sqrt{\Delta P}} = K(d_o d_i)^{0.9} \ . \tag{2-1}$$

is the same for both miniature and large hydroclones (3 to 36 inches in

diameter), except the K value increased slightly for the 10° miniature hydroclone. The larger value of K may be due to the smaller included angle and the smoother surfaces obtained with the miniature glass hydroclone. Matschke (9) felt that the good agreement between the large and miniature hydroclones strengthens the above equation.

CHAPTER III

STATEMENT OF PROBLEM

The purpose of this investigation was to develop an analytical expression to evaluate the ability of a hydroclone to eliminate contaminants from hydraulic fluid, and, after the development of this expression, to adapt it to a Donner Electrical Analog. The results from the analog were then to be compared with experimental data taken from a specific hydroclone at a fixed flow rate.

The use of an underflow pot in place of a separate discharge line from a hydroclone is a relatively new idea in the field of liquid-solid separation. However, no attempt was to be made to develop a mathematical expression for its performance.

The diameter of the maximum size particle passed by a hydroclone is the only factor which really determines its efficiency. Initiated on that basis, this investigation was carried out by comparing predicted elimination ability to filtered samples of hydraulic fluid.

CHAPTER IV

ANALYTICAL DEVELOPMENT

To predict the contaminant elimination ability of a hydroclone with an underflow pot it is necessary to know whether a contaminant particle has sufficient time to move from a position in the hydroclone near the bottom of the vortex finder to a position of greater radius in the hydroclone. Thus it will be carried past the "plane of no return" and into the underflow pot.

This development provides for an equation which can be solved in terms of time for a particle to move to a given radius.

In this analysis, the following basic assumptions were made.

1. The flow pattern predicted by Criner (2) more accurately describes the flow pattern of the fluid and the movement of the particles in a hydroclone than do other suggested flow patterns.

2. Solids move through the hydroclone assuming the velocity of the fluid at every point except where motion relative to the fluid is induced by centrifugal forces. This statement can be true only for particles of zero size and is only approximate for particles of finite size.

3. Correct application of back pressure to the underflow will eliminate the air core without loss of separation efficiency.

4. The radial acceleration of a particle in a hydroclone is large enough to be considered even though the principle acceleration is that provided by the tangential velocity.

5. Gravity and buoyant forces of a particle are small enough to be neglected.

Figure 1 shows a velocity field existing within the hydroclone boundary. The fluid is introduced tangentially at the outer boundary of the cylindrical portion and thus a two-dimensional vortex type flow configuration must exist at every axial cross section. Flow (A) illustrates this type of flow.

Figure 2, taken from Binder (11), pictures the change of tangential linear velocity, V, with respect to the radius, r, of the hydroclone. The tangential velocity, V, increases very nearly as the inverse of the radius.

$$V = \frac{K_2}{r} . \qquad (4\text{-}1)$$

The above condition is for the outer spiral which is a free vortex. The most important velocity and its distribution in a free vortex is the tangential velocity because it and the mass of a particle provide the centrifugal force for separation of solids from liquids. By the principle of the Conservation of Moment of Momentum, the flow just described is irrotational, assuming a frictionless fluid moving in a horizontal circular path with no torque applied. As long as the total energy of the system remains constant, the product, Vr, must be constant.

The point in Figure 2 where V decreases with decreasing radius is the inner radius of the outer spiral and the outer radius of the inner spiral. These spirals are shown in Figure 3. This inner spiral is a forced vortex, because a torque is applied to the body of the fluid. If each infinitesimal particle in the field of flow rotates about its own

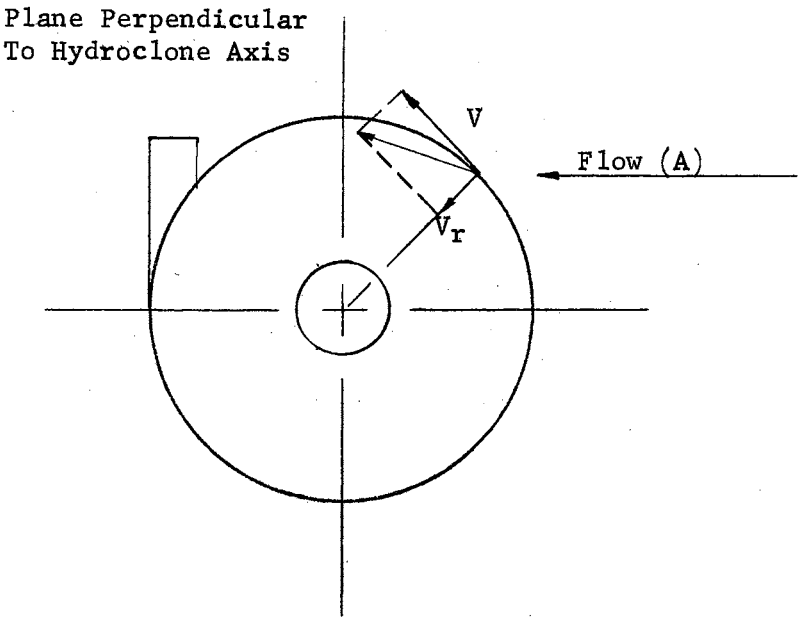

Figure 1. Velocity Field (A) In a Hydroclone

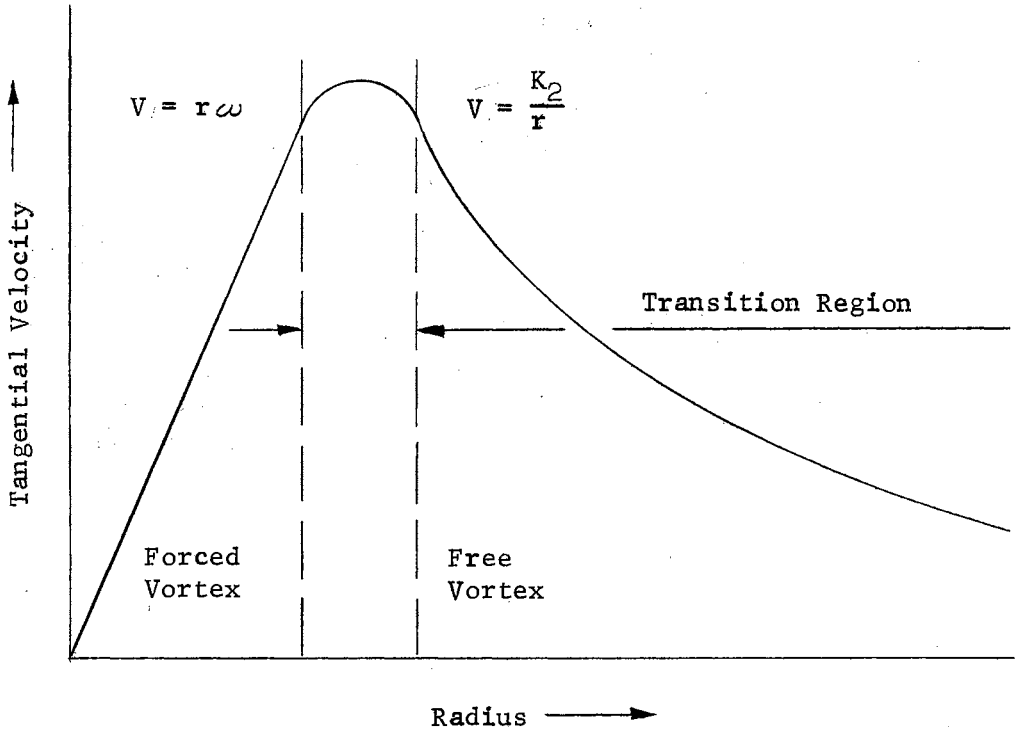

Figure 2. Tangential Velocity Distribution In a Hydroclone

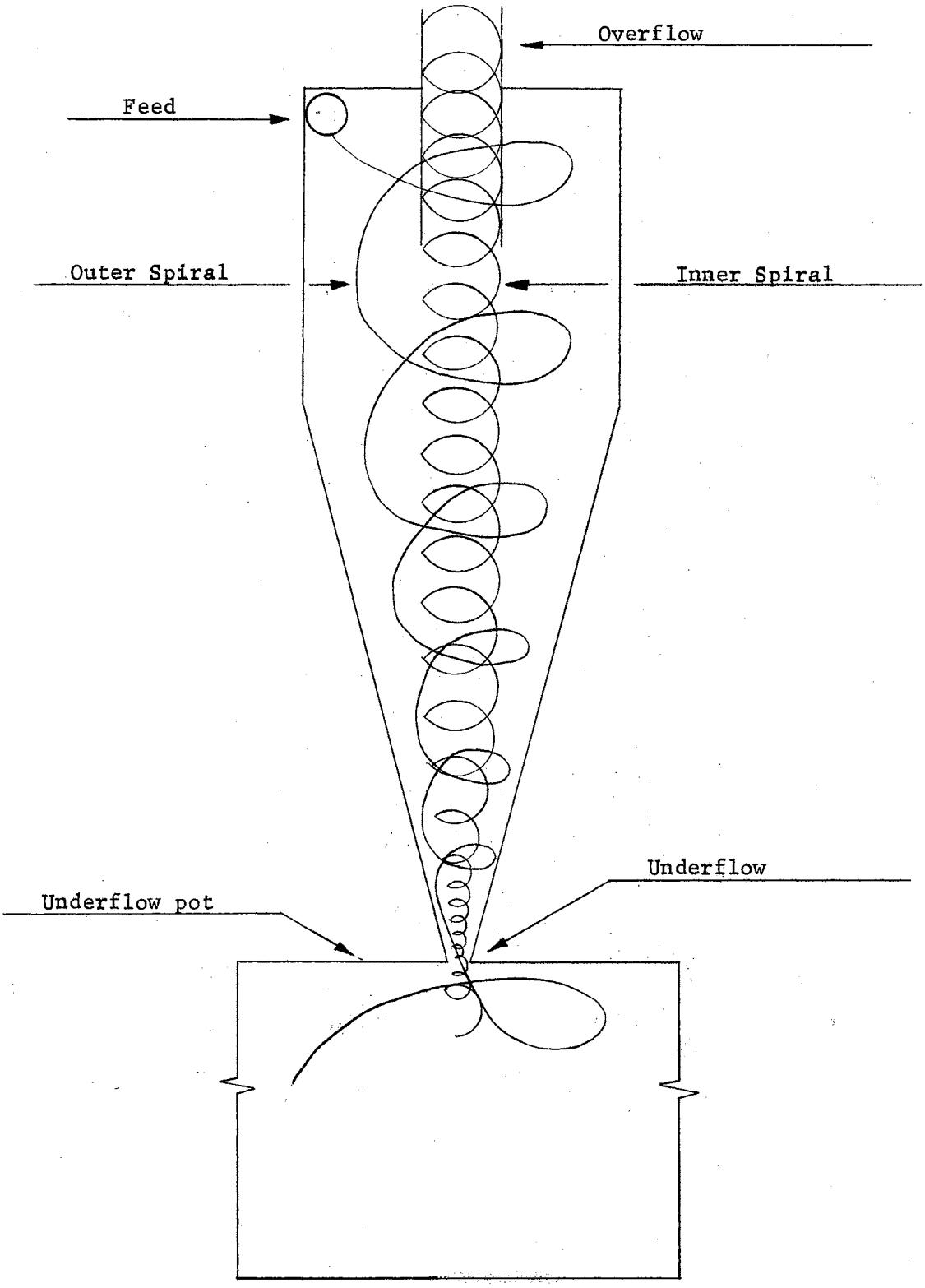

Figure 3. Flow Spirals In a Hydroclone

axis, such a flow is designated as rotational. The equation

$$V = r\omega \, . \qquad (4\text{-}2)$$

represents the tangential linear velocity at any point in the fluid in the inner spiral.

Flow energy is dissipated by random motion of the fluid elements. In the laminar flow of a fluid the energy dissipation must depend upon the rate of migration of molecules from one fluid region to another of higher or lower velocity. The molecular mixing process is constant at a constant temperature; therefore, the viscosity is constant.

If flow becomes turbulent, groups of molecules will migrate between regions in the fluid. Once the mixing process is speeded, the "eddy viscosity" becomes much larger and a function of the degree of turbulence. The effect of normal fluid viscosity is obscured if the energy losses become large due to turbulence.

There is always a radial velocity, V_r, superimposed on the vortex motion in planes perpendicular to the hydroclone axis, as the fluid is introduced at the outer wall of the hydroclone and removed at the inner spiral. The vortex strength is maintained, because the radial flow transports new fluid to the inner portion of the vortex.

The tangential velocity, V, determines the pressure generated by the vortex. If the radial flow changes along the axis of the hydroclone, then V and the radial pressure gradient must also change. No conceivable axial flow can cause a pressure gradient in the axial direction that will compare to the radial gradient shown in Figure 4. Binder (11) presented this figure in his discussion of vortexes. Thus the radial gradients must

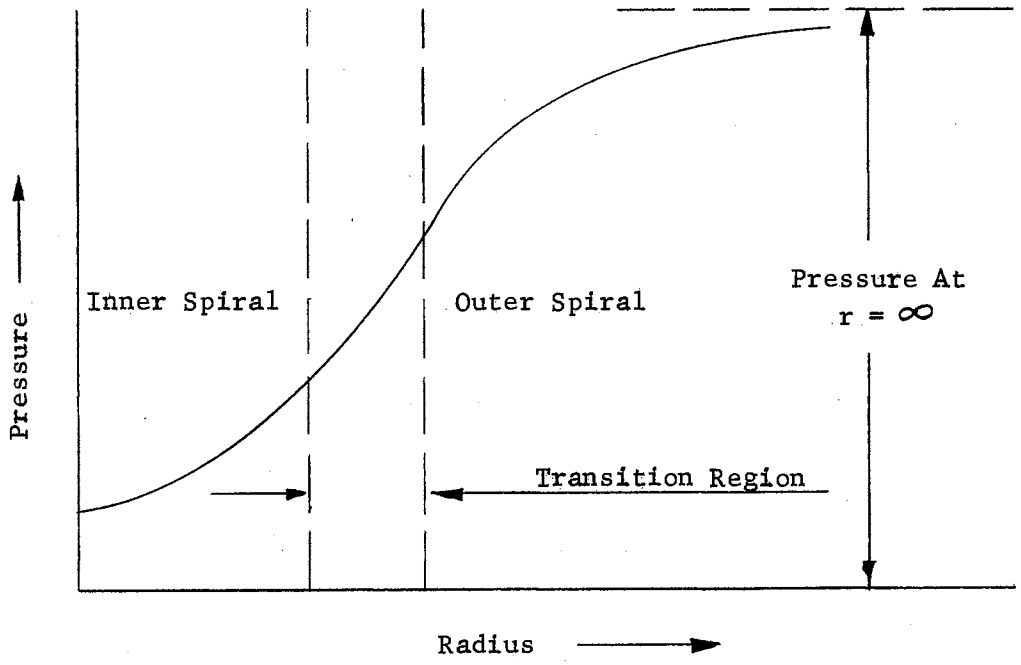

Figure 4. Pressure Distribution In a Hydroclone

be substantially constant with respect to the axial position. It may be summarized that the radial flow must be nearly independent of axial position.

The total flow to the inner spiral is proportional to the length along the axis of the hydroclone when the radial flow is constant per unit area along the axis. The vertical flow past any cross section is proportional to the vertical distance from the bottom of the cone to the cross section. Flow (B) in Figure 5 shows the vertical component, V_Z, which is a result of this flow. The velocity, V_Z, is directed toward the tip of the cone in the outer spiral and towards the overflow

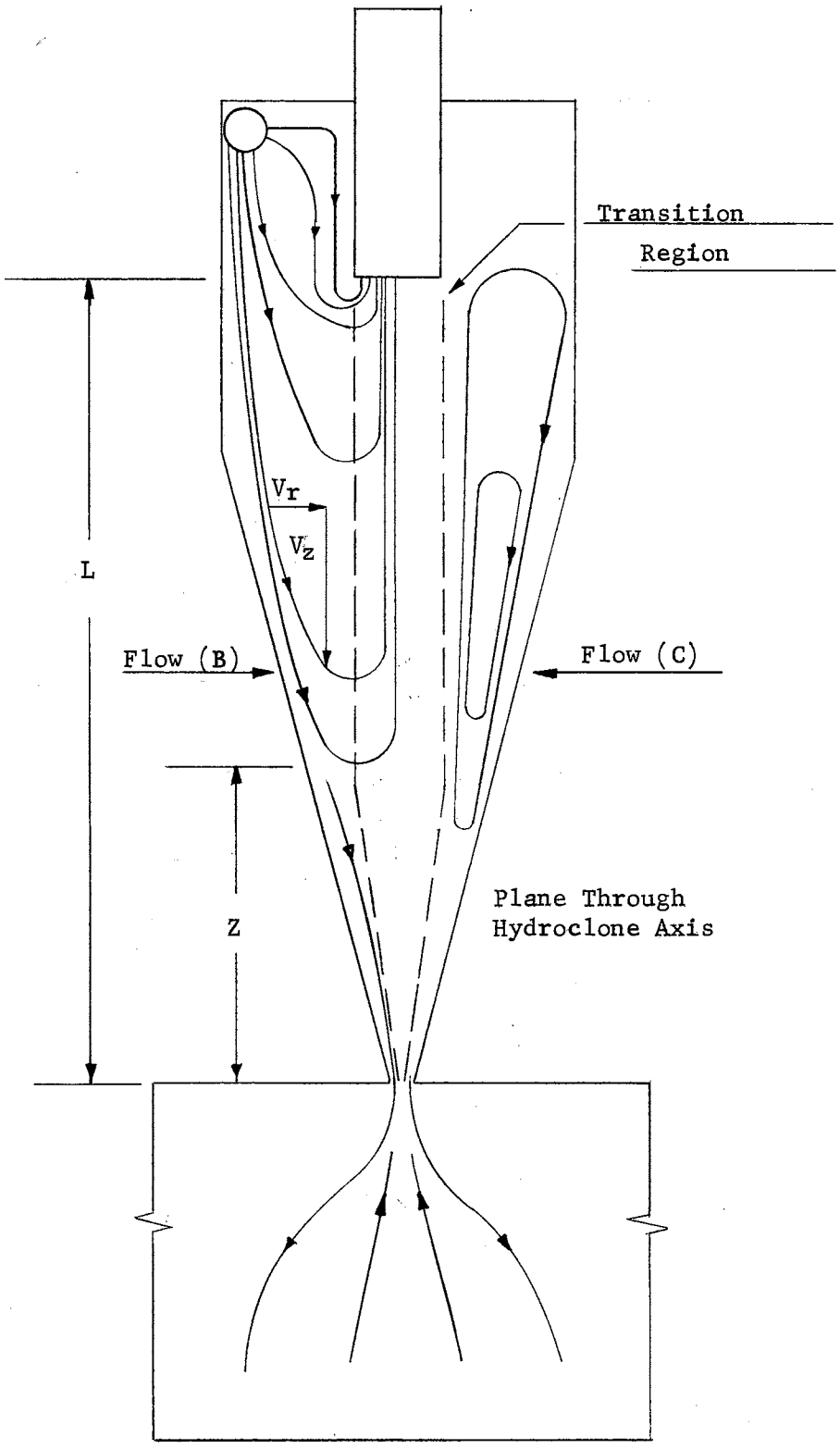

Figure 5. Velocity Fields (B) and (C) In a Hydroclone

nozzle in the inner spiral. The transition region between these two flow patterns is indicated by a dotted line in Figure 5.

The core diameter is determined by the overflow nozzle diameter and the generated head available to accelerate fluid into the inner vortex. The underflow nozzle diameter can be anything from smaller to larger than the overflow diameter. In the particular hydroclone being evaluated the underflow and overflow diameters are not the same. Cross sections of the hydroclone used in the electrical analog studies and in experimental verification are presented in Figures 6 and 7. Figure 8 is a picture of this hydroclone before assembling. A hydroclone with an underflow pot has two-way flow through the underflow nozzle. The entering fluid from the outer vortex stays to the outside of the opening. The clarified fluid upon returning to the hydroclone from the pot passes through the center of the underflow port into the inner spiral of the hydroclone. A hydroclone with a pot will allow only half as much fluid to pass through the underflow opening as one with standard underflow because an equal volume of fluid must return. In the upper portion of the hydroclone the resistance to tangential flow near the boundary wall is unimportant. The flow resistance and energy dissipation in the boundary layer is relatively high at the hydroclone cone apex, because of the small radius and the consequent large V adjacent to the wall. A flow pattern illustrated by flow (C) of Figure 5 exists, as some extra fluid must reach this region to

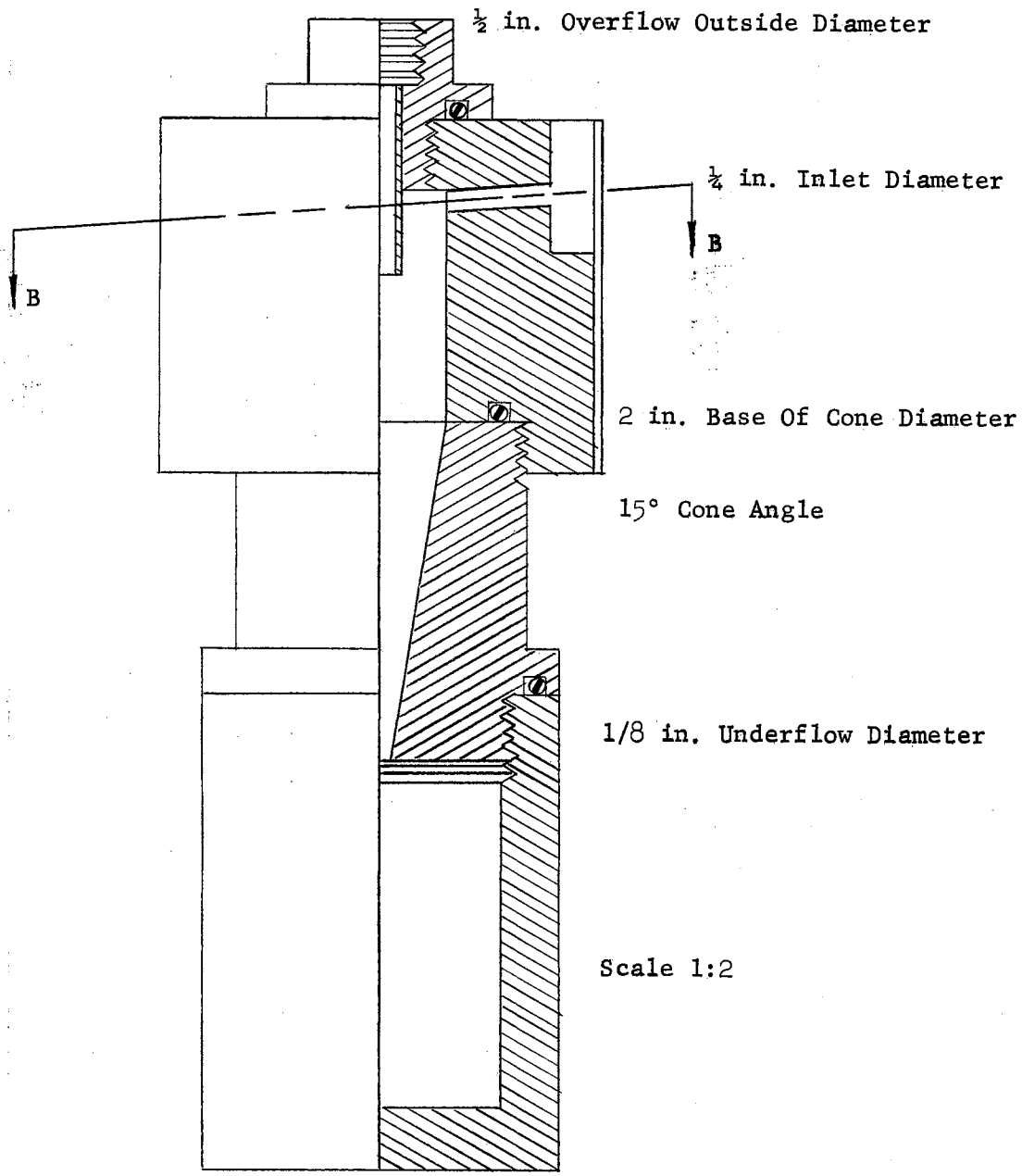

Figure 6. Hydroclone Cross Section A - A

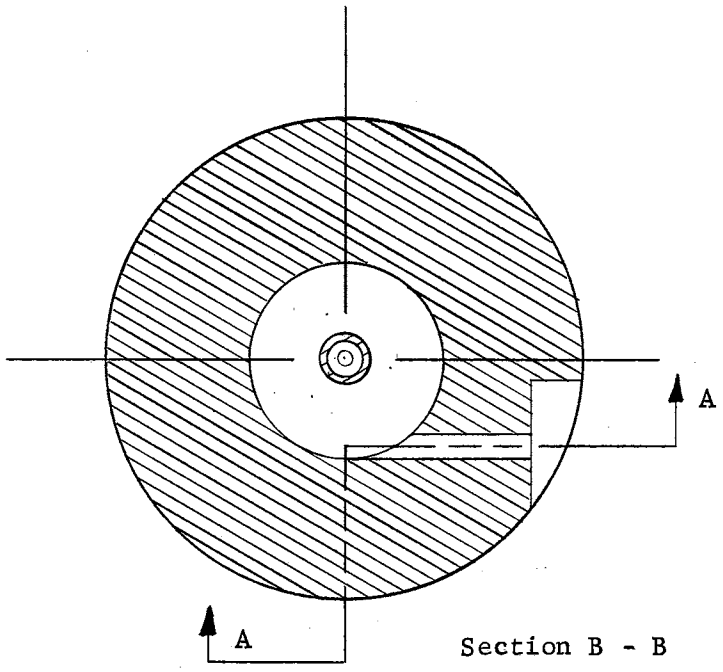

Scale 1:2

Figure 7. Hydroclone Cross Section B - B

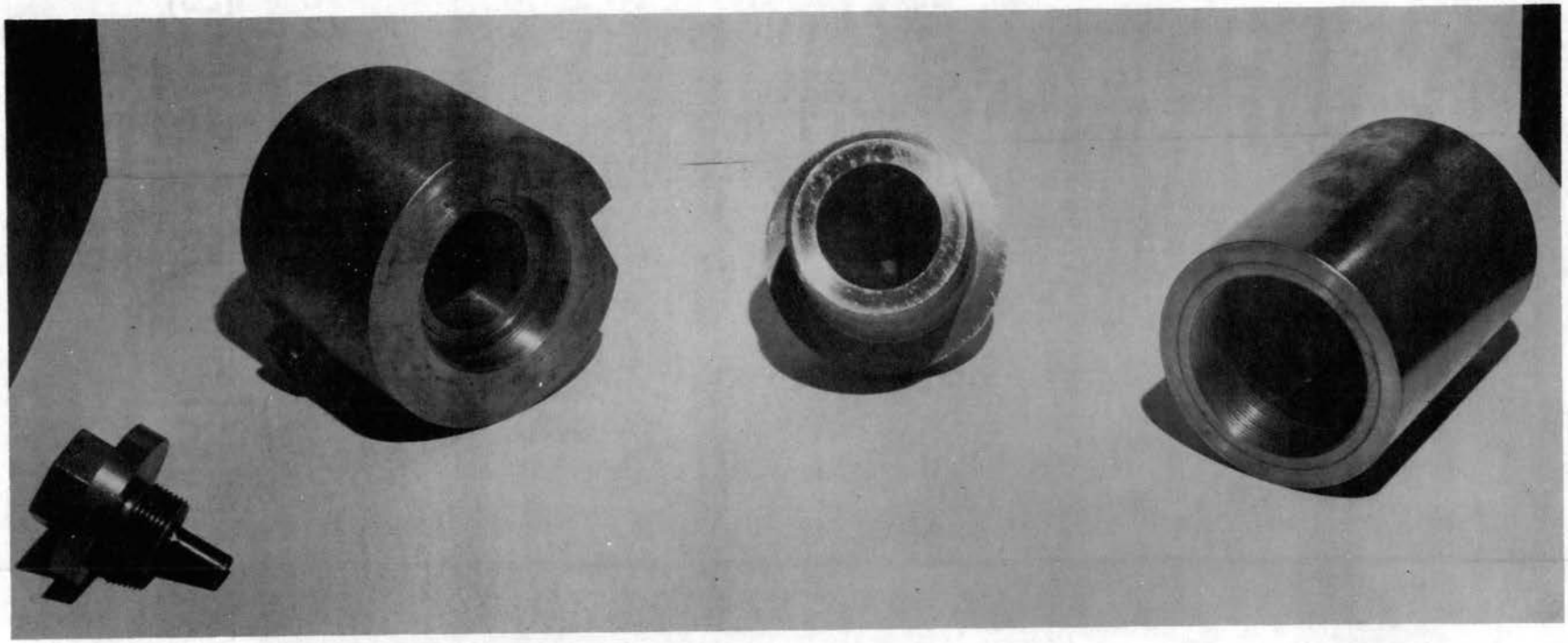

Figure 8. Hydroclone Assembly

make up for energy losses. The only effect of flow (C) on the radial velocity is to increase it in the lower portion of the hydroclone and decrease it in the upper region. The radial velocity deviates appreciably from the average value only in the very tip of the cone.

The differential equation to represent the radial movement of a particle will consider both radial and tangential velocities. The principle acceleration in the hydroclone is that provided by the tangential velocity circulating in planes perpendicular to the axis. This acceleration is numerically expressed by V^2/r. At this point, exception is taken to a statement made by Criner (2). He states that changes in V_r and V_z are not of sufficient magnitude or time duration to modify the effect of V^2/r. In the study of particle motion it is the radial position of the particle which determines whether or not it will be separated from the overflow; therefore, radial acceleration is very definitely a part of this investigation.

In the outside spiral, the particles are moved toward the core by V_r but are retarded by V^2/r. A single particle subjected to V_r and V^2/r will find a radius at which the centrifugal force on it equals the drag force. The particle will then rotate about the axis of the hydroclone at this radius. Particles of different sizes would come to rest at their respective radii with the smaller ones nearer the core.

It is with this background in mind a differential equation is developed representing the acceleration of a contaminant particle from

the outside radius of a vortex finder to some radius within the hydroclone.

The basic relation setting forth the action of a particle is the acceleration force on the particle equals the centrifugal force minus the drag force.

$$F_a = F_c - F_d. \tag{4-3}$$

Figure 9 illustrates this together with the buoyant force and the gravitational force which are neglected.

$$F_a = (\text{mass of particle})(\text{radial acceleration}) \tag{4-4}$$

$$F_a = \left[\frac{4}{3}\pi\left(\frac{D}{2}\right)^3 \rho_s\right]\frac{dV_r}{dt} \quad . \tag{4-5}$$

$$F_c = (\text{relative mass of particle})(\text{tangential acceleration}) \tag{4-6}$$

$$F_c = \left[\frac{4}{3}\pi\left(\frac{D}{2}\right)^3(\rho_s - \rho_1)\right]\frac{V^2}{r} \quad . \tag{4-7}$$

$$F_d = 3\pi\mu D V_r \quad . \tag{4-8}$$

Equation (4-8) represents Stokes' Law for viscous flow taken from Binder (11).

Equating these forces produces the differential equation which

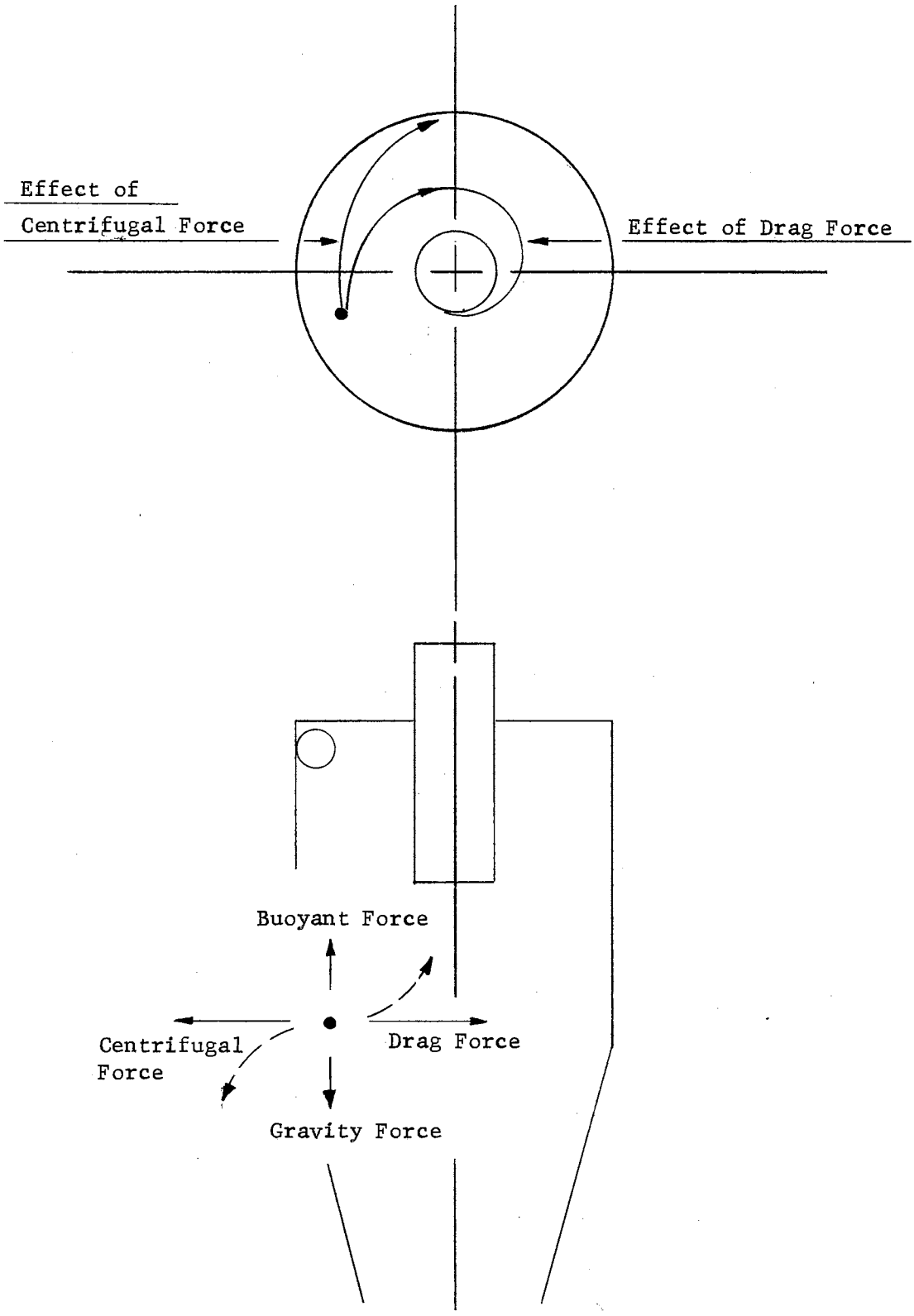

Figure 9. Forces Acting on a Particle In a Hydroclone

represents the radial movement of a particle in a hydroclone.

$$\frac{\pi D^3}{6}\rho_s\frac{dV_r}{dt} = \frac{\pi D^3}{6}(\rho_s - \rho_l)\frac{V^2}{r} - 3\pi\mu D V_r \quad . \qquad (4\text{-}9)$$

Simplifying,

$$\frac{D^2}{3}\rho_s\frac{dV_r}{dt} = \frac{D^2}{3}(\rho_s - \rho_l)\frac{V^2}{r} - 6\mu V_r \quad . \qquad (4\text{-}10)$$

Electrical analog techniques will be applied to this equation in the following chapter to simplify its practical application. First a relation for known flow patterns in a typical hydroclone is needed.

The following analytical development was needed in equation (4-10) for the tangential velocity in terms of known quantities and no new variables. The hydroclone can be reduced to a two-dimensional vortex by considering it as a section of the cone bounded by two parallel imaginary planes perpendicular to the axis of the cone. The flow in all parallel sections over or under this section will be identical to the flow in it. All flow parallel to the axis will be neglected.

The following derivation of the equation for the tangential velocity of the fluid was suggested and experimentally confirmed by Driessen (3). The basic equations for viscous fluid flow are those of Navier-Stokes as presented by Goldstein (10). Due to the physical nature of a vortex, these equations are more readily used when presented in cylindrical polar coordinates. Because the fluid is hydraulic

oil (Mil-O-5606) and the pressures encountered are not excessive (approximately 300 psi) the medium may be considered as incompressible; therefore, the mass density, ρ, is constant.

$$\frac{\partial V_r}{\partial t} + V_r \frac{\partial V_r}{\partial r} + \frac{V}{r} \frac{\partial V_r}{\partial \phi} + V_z \frac{\partial V_r}{\partial z} - \frac{V^2}{r} = \tag{4-11}$$

$$- \frac{1}{\rho} \frac{\partial P}{\partial r} + \nu \left(\nabla^2 V_r - \frac{V_r}{r^2} - \frac{2}{r^2} \frac{\partial V}{\partial \phi} \right) .$$

$$\frac{\partial V}{\partial t} + V_r \frac{\partial V}{\partial r} + \frac{V}{r} \frac{\partial V}{\partial \phi} + V_z \frac{\partial V}{\partial z} + \frac{V_r V}{r} = \tag{4-12}$$

$$- \frac{1}{\rho} \frac{1}{r} \frac{\partial P}{\partial \phi} + \nu \left(\nabla^2 V + \frac{2}{r^2} \frac{\partial V_r}{\partial \phi} - \frac{V}{r^2} \right) .$$

$$\frac{\partial V_z}{\partial t} + V_r \frac{\partial V_z}{\partial r} + \frac{V}{r} \frac{\partial V_z}{\partial \phi} + V_z \frac{\partial V_z}{\partial z} = - \frac{1}{\rho} \frac{\partial P}{\partial z} + \nu \nabla^2 V_z . \tag{4-13}$$

$$\nabla^2 \equiv \frac{\partial^2}{\partial r^2} + \frac{1}{r} \frac{\partial}{\partial r} + \frac{1}{r^2} \frac{\partial^2}{\partial \phi^2} + \frac{\partial^2}{\partial z^2} . \tag{4-14}$$

Equations (4-11), (4-12), (4-13), and (4-14) can be considerably simplified by applying limiting conditions. Only equations (4-12) and (4-14) will be used in this analysis. The limiting conditions will be listed as follows:

(a) Steady flow exists in a hydroclone; therefore, the derivatives with regard to time are zero.

$$\frac{\partial V}{\partial t} = 0 .$$

(b) Because of axial symmetry, all velocities and pressures are equal along the surface of the coaxial cylinders. Hence, velocities and pressures do not change with respect to changes in the coordinate, ϕ.

$$\frac{\partial V_r}{\partial \phi} = \frac{\partial V}{\partial \phi} = \frac{\partial P}{\partial \phi} = 0 \quad .$$

(c) As only two-dimensional flow is considered, all changes with respect to Z are null. The vertical velocity, V_z, is equal to zero.

Therefore,

$$V_z = 0 \quad ,$$

and

$$\frac{\partial V}{\partial z} = 0 \quad .$$

After applying these simplifications

$$V_r \frac{\partial V}{\partial r} + \frac{V_r V}{r} = \nu\left(\nabla^2 V - \frac{V}{r^2}\right) \quad , \qquad (4\text{-}15)$$

where

$$\nabla^2 = \frac{\partial^2}{\partial r^2} + \frac{1}{r} \frac{\partial}{\partial r} \quad . \qquad (4\text{-}16)$$

Replacing the partial derivatives by ordinary derivatives and substituting for ∇^2,

$$V_r \frac{dV}{dr} + \frac{V_r V}{r} = \nu \left(\frac{d^2V}{dr^2} + \frac{1}{r} \frac{dV}{dr} - \frac{V}{r^2} \right) . \qquad (4\text{-}17)$$

Reducing equation (4-17),

$$\frac{V_r}{r} \frac{d(Vr)}{dr} = \nu \frac{d}{dr} \left[\frac{1}{r} \frac{d(Vr)}{dr} \right] . \qquad (4\text{-}18)$$

Because of the condition of steady flow of an incompressible fluid, the continuity equation relates the mean radial velocity to the normal cross-sectional flow area as follows,

$$V_r r = K_3 . \qquad (4\text{-}19)$$

Using $V_r r = K_3 = - \frac{A}{2\pi}$ in equation (4-18) yields

$$- \frac{A}{2\pi r^2} \frac{d(Vr)}{dr} = \nu \frac{d}{dr} \left[\frac{1}{r} \frac{d(Vr)}{dr} \right] . \qquad (4\text{-}20)$$

As the radial flow in each coaxial cylinder is constant,

$$V_r r = - \frac{A}{2\pi} ; \qquad (4\text{-}21)$$

therefore,

$$A = -2\pi r V_r(1) \quad . \tag{4-22}$$

The negative sign indicates a centripetal or negative radial flow. Therefore, a negative sign occurs in equation (4-22) because "A" is considered as positive.

The differential equation (4-20) will be used to represent two-dimensional flow of an incompressible viscous fluid in a vortex. Integration of equation (4-20) can be completed resulting in the establishment of a relation between the tangential velocity and the radius.

First of all $\frac{d(Vr)}{dr}$ can be considered as a function of r.

$$\frac{d(V_r)}{dr} = f(r) \quad . \tag{4-23}$$

When the above equation is introduced in equation (4-20) the result is

$$-\frac{A}{2\pi r^2} f(r) = \nu \frac{d}{dr} \left[\frac{1}{r} f(r)\right] \quad . \tag{4-24}$$

Expanding equation (4-24) yields

$$-\frac{A}{2\pi} f(r) = \nu r \frac{df(r)}{dr} - \nu f(r) \quad . \tag{4-25}$$

Reducing the above equation further,

$$\frac{d\,f(r)}{f(r)} = \left[-\frac{A}{2\pi\nu} + 1 \right] \frac{dr}{r} \quad . \qquad (4\text{-}26)$$

The kinematic viscosity, ν, will be designated by β, coefficient of turbulent viscosity, for the remainder of this thesis.

If from equation (4-26), "n" is arbitrarily set equal to

$$-\frac{A}{2\pi\beta} + 1 \quad .$$

for a special case n = -1, then the coefficient of turbulent viscosity, β, will equal $\frac{A}{4\pi}$.

This special case n = -1 is used because it agrees best with experimental measurements conducted by Driessen (3). The concept of coefficient of turbulent viscosity, β, was proposed about 1877 by Boussinesq, and later in 1895 by Osborne Reynolds, who introduced a coefficient, $\bar{\mu}$, of molar, mechanical, or turbulent viscosity in the place of μ.

Equation (4-26) can now be integrated. With "n" in place of

$$-\frac{A}{2\pi\beta} + 1 \quad ,$$

it follows that

$$\frac{df(r)}{f(r)} = n\,\frac{dr}{r} \quad . \qquad (4\text{-}27)$$

It integrates to

$$\ln f(r) = n \ln r + \ln C_3 = \ln C_3 r^n \quad , \qquad (4\text{-}28)$$

or

$$f(r) = \frac{d(Vr)}{dr} = C_3 r^n \quad . \tag{4-29}$$

Applying the condition set forth by experimental verification that n = -1, then

$$\frac{d(Vr)}{dr} = C_3 r^{-1} = \frac{C_3}{r} \quad . \tag{4-30}$$

Multiplying and dividing the right side by dr and setting it equal to its logarithmic form yields,

$$\frac{C_3}{dr} \frac{dr}{r} = \frac{C_3 d(\ln r)}{dr} \quad . \tag{4-31}$$

Substituting equation (4-31) for equation (4-30) and integrating results in

$$\frac{d(Vr)}{dr} = \frac{C_3 d(\ln r)}{dr} \quad , \tag{4-32}$$

or

$$Vr = (C_3 \ln r + C_4) \quad , \tag{4-33}$$

or

$$V = \frac{1}{r}(C_3 \ln r + C_4) \quad . \tag{4-34}$$

Equation (4-34) is the solution of the differential equation representing two dimensional flow of an incompressible viscous fluid in a vortex for the special case of n = -1.

In order to evaluate the constants in equation (4-34) Driessen (3) used the following boundary conditions: when $r = r_2$, then $V = V_2$; when $r = r_1$, then $\frac{dV}{dr} = 0$.

The tangential velocity, V_2, is at the radius, r_2, of the cylindrical portion of the hydroclone. At the inner radius of the outer spiral and the outer radius of the inner spiral represented by r_1, the boundary condition, $\frac{dV}{dr}$, is equal to zero.

Substituting these boundary conditions into equation (4-34) yields the values of the constants C_3 and C_4.

Using $V = V_2$ when $r = r_2$,

$$V_2 = \frac{1}{r_2}(C_3 \ln r_2 + C_4) \quad . \tag{4-35}$$

Differentiating equation (4-34) yields

$$\frac{dV}{dr} = \frac{C_3}{r^2} - \frac{(C_3 \ln r + C_4)}{r^2} \quad , \tag{4-36}$$

and applying $\frac{dV}{dr} = 0$ when $r = r_1$ then

$$C_3 (1 - \ln r_1) - C_4 = 0 \quad , \tag{4-37}$$

and

$$C_3 = \frac{C_4}{(1 - \ln r_1)} \quad . \tag{4-38}$$

Thus combining equation (4-35) and (4-38) and simplifying,

$$C_3 = \frac{V_2 r_2}{1 + \ln \frac{r_2}{r_1}} \tag{4-39}$$

Final substitutions can now be made by combining equations (4-34), (4-38), and (4-39).

$$V = \frac{1}{r} \frac{V_2 r_2 (\ln r)}{1 + \ln \frac{r_2}{r_1}} + \frac{1}{r} \frac{V_2 r_2 (1 - \ln r_1)}{1 + \ln \frac{r_2}{r_1}} \tag{4-40}$$

or

$$V = \frac{V_2 r_2}{r} \left[\frac{1 + \ln \frac{r}{r_1}}{1 + \ln \frac{r_2}{r_1}} \right] \quad . \qquad (4\text{-}41)$$

Equation (4-41) can now be substituted into equation (4-10) yielding the final form ready for application to a specific hydroclone.

CHAPTER V

APPLICATION OF ELECTRICAL ANALOG

Before equation (4-10) is solved using the Donner Analog Computer, it is reduced by evaluating many of its terms from fixed conditions of the hydroclone. This solution is for a flow rate of 8 gpm in the hydroclone shown in Figures 6 and 7. The only variable to be changed will be the diameter of the glass beads. Their size will range from Type I (50-micron average) to Type II (29-micron average) according to Table I.

$$\frac{D^2}{3}\rho_s \frac{dV_r}{dt} = \frac{D^2}{3}(\rho_s - \rho_l)\frac{V^2}{r} - 6\mu V_r \quad . \tag{4-10}$$

where

$D = 0.001967$ in., Type I glass beads

$D = 0.001140$ in., Type II glass beads

$\rho_s = 0.0904$ lb per cu in., mass density of Type I and Type II glass beads.

$\nu = 20$ centistokes @ 80°F for Mil-O-5606 hydraulic fluid.

specific gravity = 0.8555 for Mil-O-5606 hydraulic fluid.

$\rho_l = 0.0309$ lb per cu in., mass density of Mil-O-5606 hydraulic fluid.

μ = (specific gravity)(ν).

$\mu = (0.8555)(20) = 17.11$ centipoises.

1 Reyn = 1 lb (Force) sec per sq in.

1 Reyn = (1.45×10^{-7})(1 centipoise).

$\mu = (1.45 \times 10^{-7})(17.11) = 2.48 \times 10^{-6}$ lb sec per sq in.

TABLE I

GLASS BEAD DATA

Diameter

	Minimum	Maximum	Average
Microns*			
Type I	31	69	50
Type II	18	40	29
Inches			
Type I			0.001969
Type II			0.001140

Approximately 90% by weight of these beads will fall within the specified size range.

Occasional flaws or bubbles will cause some variation in the density of individual beads. The density will decrease slightly in the finer bead sizes.

*Note: The term 'micron' is derived from the metric system of measurement and represents a size or distance equal to one millionth of a meter or approximately 0.00003937ths of an inch.

Simplifying equation (4-10),

$$\frac{\rho_s}{3}\frac{d^2r}{dt^2} = \frac{(\rho_s-\rho_l)}{3}\frac{V^2}{r} - \frac{6\mu}{D^2}\frac{dr}{dt} \quad . \tag{5-1}$$

Substituting

$$\frac{(0.0909)}{3}\frac{d^2r}{dt^2} = \frac{(0.0904 - 0.0309)}{3}\frac{V^2}{r} - \frac{(6)(2.48\times10^{-6})(32.2)(12)}{D^2}\frac{dr}{dt} \tag{5-2}$$

Reducing,

$$\frac{d^2r}{dt^2} = 0.658\frac{V^2}{r} - \frac{5.32\times10^{-3}}{D^2}\frac{dr}{dt} \quad . \tag{5-3}$$

The tangential velocity can now be evaluated using equation (4-41):

$$V = \frac{V_2 r_2}{r}\left[\frac{1 + \ln\frac{r}{r_1}}{1 + \ln\frac{r_2}{r_1}}\right] \quad . \tag{4-41}$$

where, from Figure 6 of the hydroclone,

$r_1 = \frac{1}{2}(0.50) = 0.25$ in.

$r_2 = \frac{1}{2}(2.0) = 1.0$ in.

$d_i = 0.250$ in.

$A_i = \frac{\pi d_i^2}{4} = \frac{\pi(0.250)^2}{4} = 0.0491$ sq in.

$Q = 30.8$ cu in. per sec (8 gpm).

$V_2 = \frac{Q}{A_i} = \frac{30.8}{0.0491} = 628$ in. per sec.

Substituting,

$$V = \left[\frac{(628)(1)}{r}\right]\left[\frac{1 + \ln r - \ln 0.25}{1 + \ln\frac{1}{0.25}}\right] \tag{5-4}$$

Reducing,

$$V = \frac{(263)}{r}(2.385 + \ln r) \quad . \tag{5-5}$$

Substituting equation (5-5) in equation (5-3) yields

$$\frac{d^2r}{dt^2} = \frac{4.56 \times 10^4}{r^3}(2.385 + \ln r)^2 - \frac{5.32 \times 10^{-3}}{D^2} \frac{dr}{dt} \quad (5\text{-}6)$$

Let

$$f(r) = \frac{4.56 \times 10^4}{r^3}(2.385 + \ln r)^2 \quad (5\text{-}7)$$

Then

$$\frac{d^2r}{dt^2} = f(r) - \frac{5.32 \times 10^{-3}}{D^2} \frac{dr}{dt} \quad (5\text{-}8)$$

Table II lists f(r) for the radius, r, ranging from $r_1 = 0.00$ to $r_2 = 1.00$.

To apply the electrical analog f(r) must be scaled on the Donner Variable Base Function Generator, Model 3750. Because the function generator approximates the curve of a function with a series of connected straight line segments, a plot must be made of the function in terms of volts for both the x and y axis. Figure 10 is a plot of f(r) vs. radius, r.

Because 100 volts is the maximum range of the analog computer the following scale factors were developed:

$$\text{Y scale factor} = \frac{100}{3.433 \times 10^6} = 2.91 \times 10^{-5} \text{ volts/unit f(r)}$$

$$\text{X scale factor} = \frac{100}{1.00} = 100 \text{ volts/unit r}$$

Table III represents the x and y voltages plotted in Figure 11. These same x and y voltages are in turn set on the function generator by adjusting one set of break voltage controls and the corresponding slope controls. Because the slope of f(r) exceeded the limit of the slope control at point x = 25 volts, it was necessary to establish two line

TABLE II

FUNCTION(r) DATA

$$f(r) = \frac{4.56 \times 10^6}{r^3} (2.385 + \ln r)^2$$

r(inches)	f(r)
0.00	Indeterminate
0.092	0.000
0.20	3.433×10^6
0.25	2.917×10^6
0.40	1.537×10^6
0.55	8.749×10^5
0.70	4.943×10^5
0.85	3.661×10^5
1.00	2.594×10^5

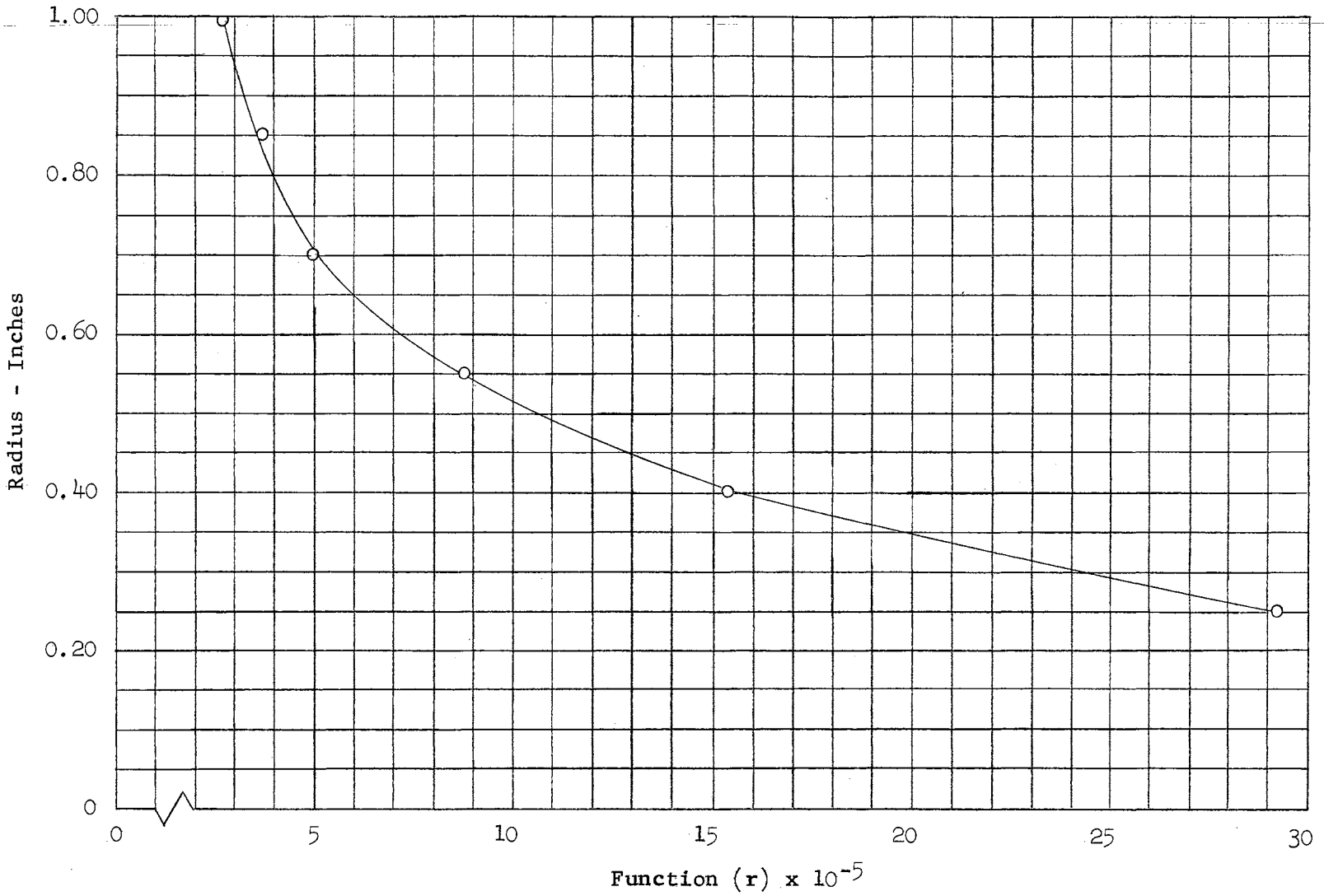

Figure 10. Function (r) Plot

TABLE III

FUNCTION GENERATOR DATA

r (inches)	x (volts)	x-20 (volts)	y (volts)	Point	Line Segments
0.20	20	0	100	none	none
0.25	25	5	84.9	1 & 2	2
0.40	40	20	44.7	3	1
0.55	55	35	25.5	4	1
0.70	70	50	14.4	5	1
0.85	85	65	10.7	6	1
1.00	100	80	7.6	7	1

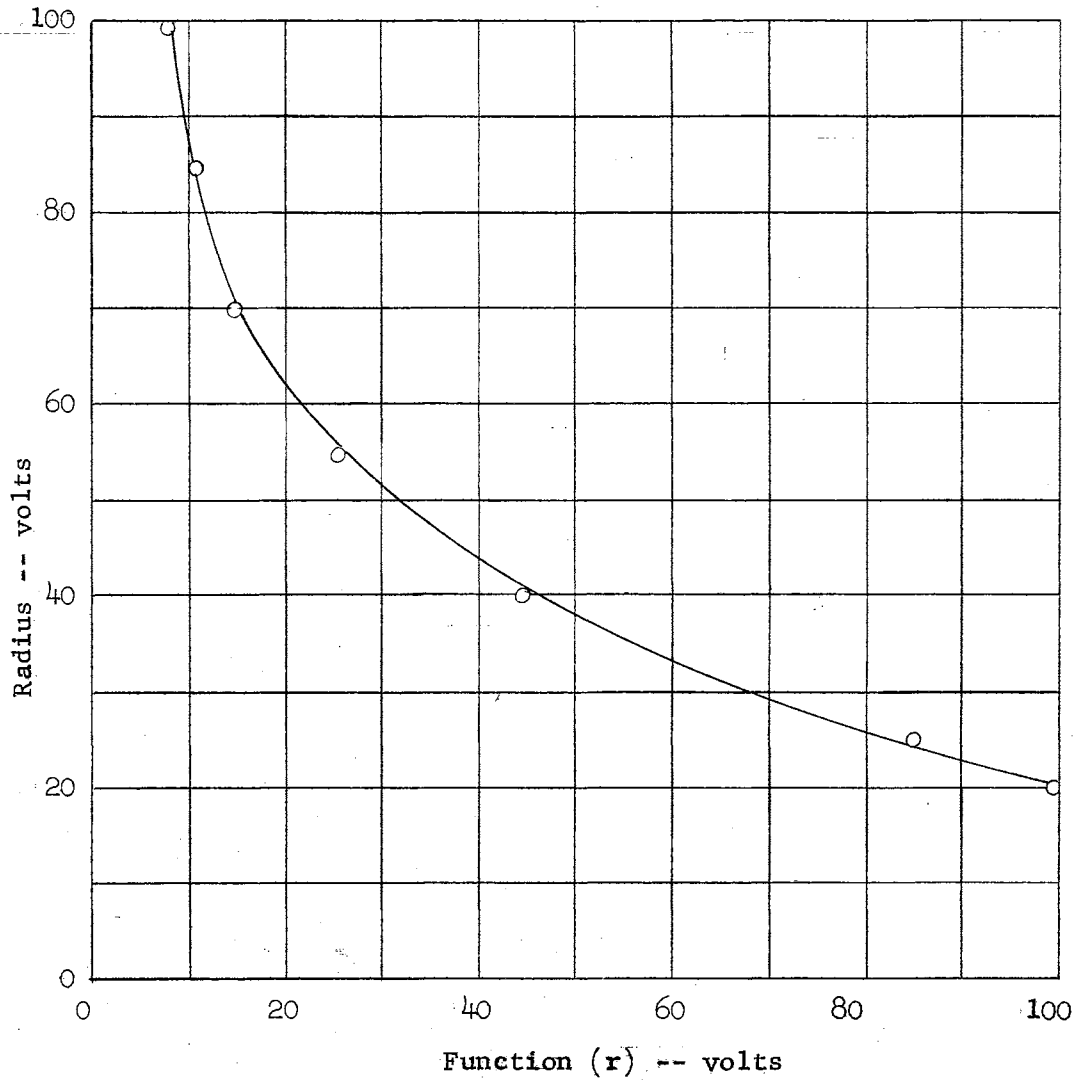

Figure 11. Function Generator Plot

segments for the same points.

For D = 50 microns in equation (5-8),

$$\frac{d^2r}{dt^2} = f(r) - 1.375\times10^3 \frac{dr}{dt} \quad . \tag{5-9}$$

For D = 29 microns in equation (5-8),

$$\frac{d^2r}{dt^2} = f(r) - 4.09\times10^3 \frac{dr}{dt} \quad . \tag{5-10}$$

To program equations (5-9) and (5-10) on the analog the only difference will be an appropriate potentiometer setting providing for D = 29 microns and D = 50 microns; therefore, only equation (5-9) will be used as an example.

Again scaling is necessary to determine the electrical components to use on the electrical analog problem board.

$\overline{r}$ = electrical equivalent.

$\overline{\frac{dr}{dt}}$ = electrical equivalent.

$\overline{\frac{d^2r}{dt^2}}$ = electrical equivalent.

$\overline{f(r)}$ = electrical equivalent.

α_1 = scale factor for $\overline{\frac{d^2r}{dt^2}}$.

α_2 = scale factor for $\overline{\frac{dr}{dt}}$.

α_3 = scale factor for $\overline{f(r)}$.

α_4 = scale factor for $\overline{r}$.

α_t = scale factor for time.

One hundred volts is used as maximum range for $\overline{r}$, $\overline{\frac{dr}{dt}}$ and $\overline{\frac{d^2r}{dt^2}}$.

Application of these scale factors to equation (5-9) results in

$$\alpha_t \alpha_1 \frac{\overline{d^2r}}{dt^2} = \alpha_3 \overline{f(r)} - \alpha_2 1.375 \times 10^3 \frac{\overline{dr}}{dt} \quad . \tag{5-11}$$

$$\frac{\overline{dr}}{dt} = \frac{1}{\alpha_t} \int_0^{\bar{r}} \left[\frac{\alpha_3}{\alpha_1} \overline{f(r)} - \frac{\alpha_2}{\alpha_1} 1.375 \times 10^{-3} \frac{\overline{dr}}{dt} \right] \quad . \tag{5-12}$$

Also applying these scale factors to the radius, r, results in

$$\alpha_t \alpha_4 \bar{r} = \int_0^{\bar{r}} \alpha_2 \frac{\overline{dr}}{dt} \quad , \tag{5-13}$$

and

$$\bar{r} = \frac{\alpha_2}{\alpha_t \alpha_4} \int_0^{\bar{r}} \frac{\overline{dr}}{dt} \quad . \tag{5-14}$$

Solving for the scale factors,

$$\frac{d^2r}{dt^2} = \alpha_1 \frac{\overline{d^2r}}{dt^2} \quad . \tag{5-15}$$

$$\frac{dr}{dt} = \alpha_2 \frac{\overline{dr}}{dt} \quad . \tag{5-16}$$

$$f(r) = \alpha_3 \overline{f(r)} \quad . \tag{5-17}$$

$$r = \alpha_4 \bar{r} \quad . \tag{5-18}$$

Assumptions

$\left[\frac{d^2r}{dt^2}\right]$ max = 100 in. per sec per sec, and $\frac{\overline{d^2r}}{dt^2}$ = 100 volts.

$\left[\frac{dr}{dt}\right]$ max = 1000 in/per sec and $\overline{\frac{dr}{dt}}$ = 100 volts.

$\overline{f(r)}$ = 100 volts.

(r) max = 1.00 in. and $\bar{r}$ = 100 volts.

1 second in problem = 104 seconds on computer.

From the above assumptions the scale factors can be found.

$$\alpha_1 = \frac{\left[\frac{d^2r}{dt^2}\right]_{MAX}}{\left[\overline{\frac{d^2r}{dt^2}}\right]} = \frac{100}{100} = 1 \quad .$$

$$\alpha_2 = \frac{\left[\frac{dr}{dt}\right]_{MAX}}{\left[\overline{\frac{dr}{dt}}\right]} = \frac{1000}{100} = 10 \quad .$$

$$\alpha_3 = \frac{f(r)_{MAX}}{\overline{f(r)}} = \frac{2.917 \times 10^6}{100} = 2.917 \times 10^4 \quad .$$

$$\alpha_4 = \frac{(r)_{MAX}}{\bar{r}} = \frac{1}{100} = 0.01 \quad .$$

$$\alpha_t = 10^4 \quad .$$

The values of the resistors and the capacitors for integrators 1 and 2 of the circuit shown in Figure 12 can be found using the scale factors.

Because the integrator has a feedback, C_a is the common capacitor for resistances R_{e1} and R_{e2}. The potentiometer readings for potentiometers P_{o1}, P_{o2}, and P_{o3} are determined at this time also.

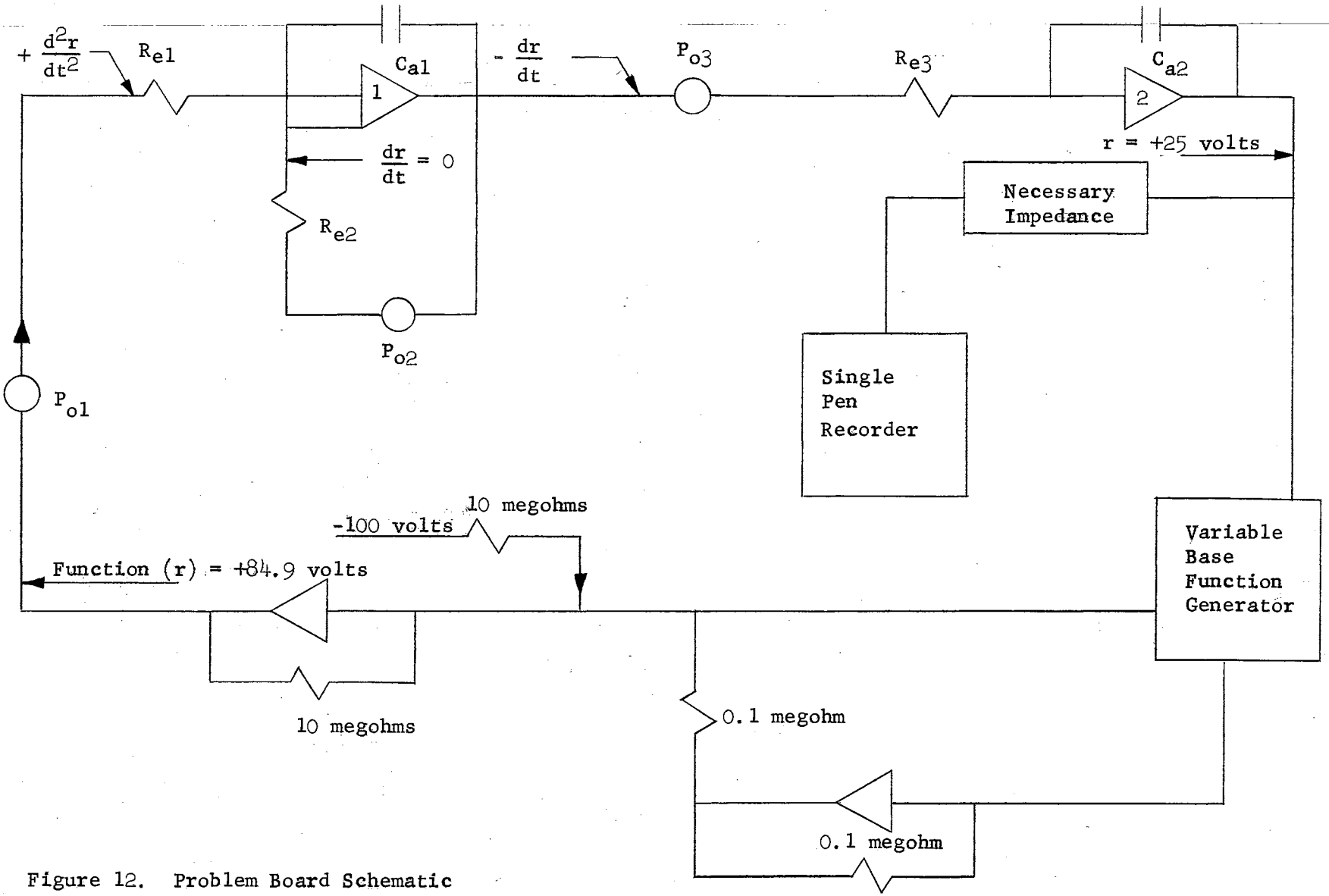

Figure 12. Problem Board Schematic

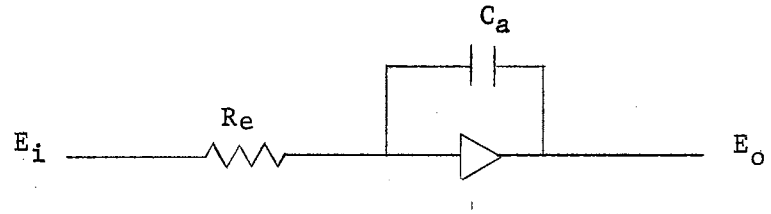

Figure 13. Electrical Integrator Circuit Schematic

$$E_o \doteq -\frac{1}{RC}\int_o^t E_i \, dt \quad . \tag{5-19}$$

Figure 13 and equation (5-19) represent an electrical analog integrator.

$$\frac{P_{o1}}{R_{e1}C_{a1}} = \frac{\alpha_3}{\alpha_1 \alpha_t} = \frac{2.917 \times 10^4}{(1)(10^4)} \quad .$$

Let R_{e1} = 10 megohm

C_{a1} = .01 mfd.

Therefore

P_{o1} = (2.917)(10)(.01) = 0.2917.

$$\frac{P_{o2}}{R_{e2}C_{a1}} = \frac{1.375 \times 10^3 \ \alpha_2}{\alpha_t \ \alpha_1} = \frac{(1.375 \times 10^3)(10)}{(10^4)(1)} \quad .$$

Let R_{e2} = 10 megohm

C_{a1} = .01 mfd.

Therefore

P_{o2} = (1.375)(10)(.01) = 0.1375

$$\frac{P_{o3}}{R_{e3}C_{a2}} = \frac{\alpha_2}{\alpha_4 \alpha_t} = \frac{10}{(10^4)(10^{-2})} \quad .$$

Let R_{e3} = 1 megohm

$$C_{a2} = 1 \text{ mfd.}$$

Therefore

$$P_{o3} = (.1)(1)(1) = .1.$$

The circuit shown in Figure 12 is set on the analog problem board.

A read-out of the plots of radius, r, vs. time, t, is made with a Recti/Riter one-pen recorder operating at a rate of one foot per minute. Figures 14 and 15 are drawings of these plots. From these plots an evaluation of a specific hydroclone with a flow of 8 gpm using Type I and Type II glass beads is possible. Figure 16 is a picture of the electrical analog computer and the recorder that were used.

The physical reaction of a glass bead can be easily noted. The larger particle (D = 50 microns) attained a greater radius in the hydroclone in much less time than did the smaller particle (D = 29 microns). This explains why separation ability is so much greater with the large glass beads. Chapter VI provides experimental verification that the separation ability is higher with larger glass beads. The fact that a greater radius is reached quicker with a larger glass bead in planes near the bottom of the vortex finder and perpendicular to the axis helps prevent short-circuiting of the particles from the inlet nozzle directly to the overflow. Short-circuiting does not allow for the particles to separate from the feed stream, because they leave at the vortex finder rather than follow the outer spiral to the "plane of no return" and thus to the underflow pot.

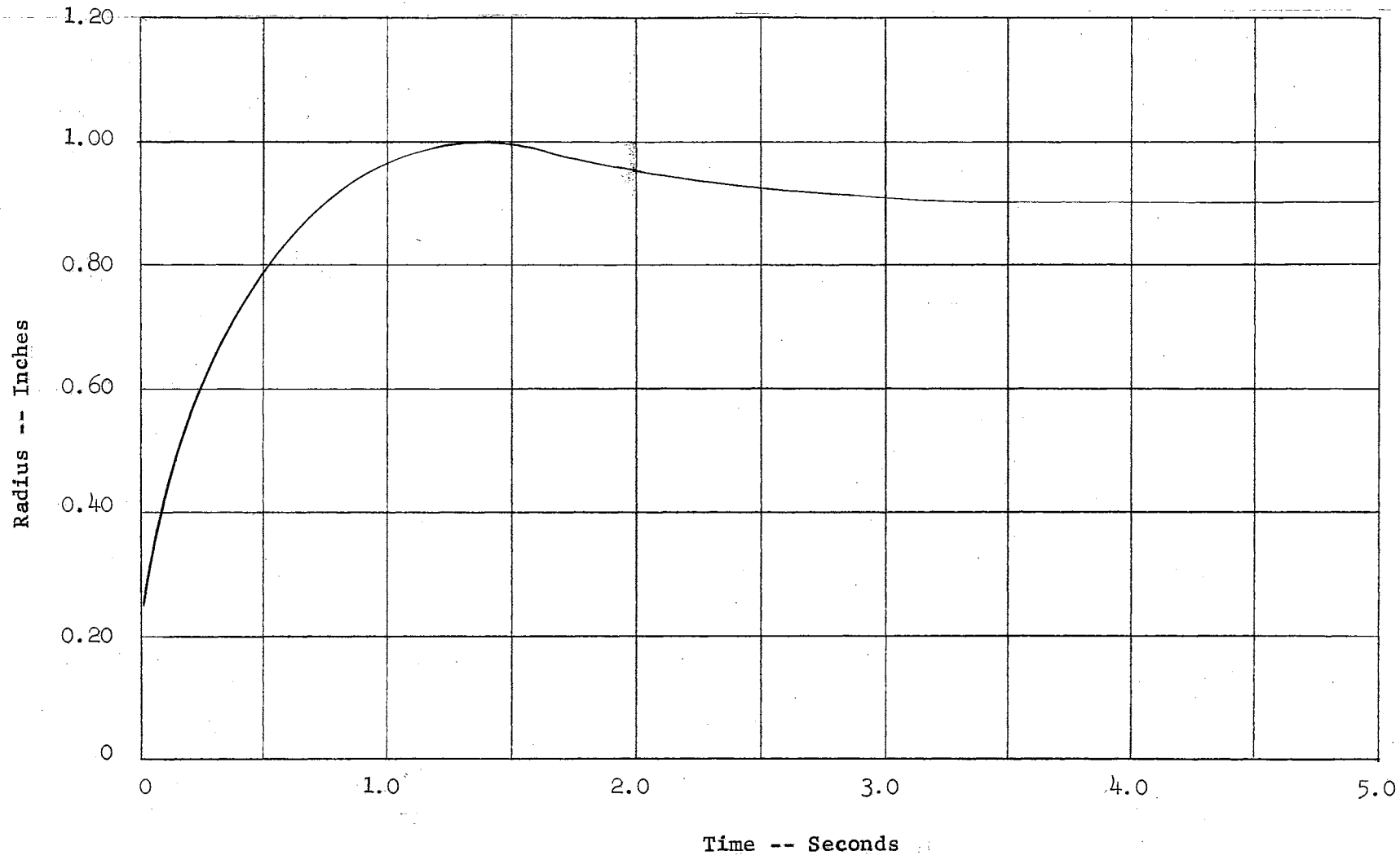

Figure 14. Separation Plot (Type I Glass Beads)

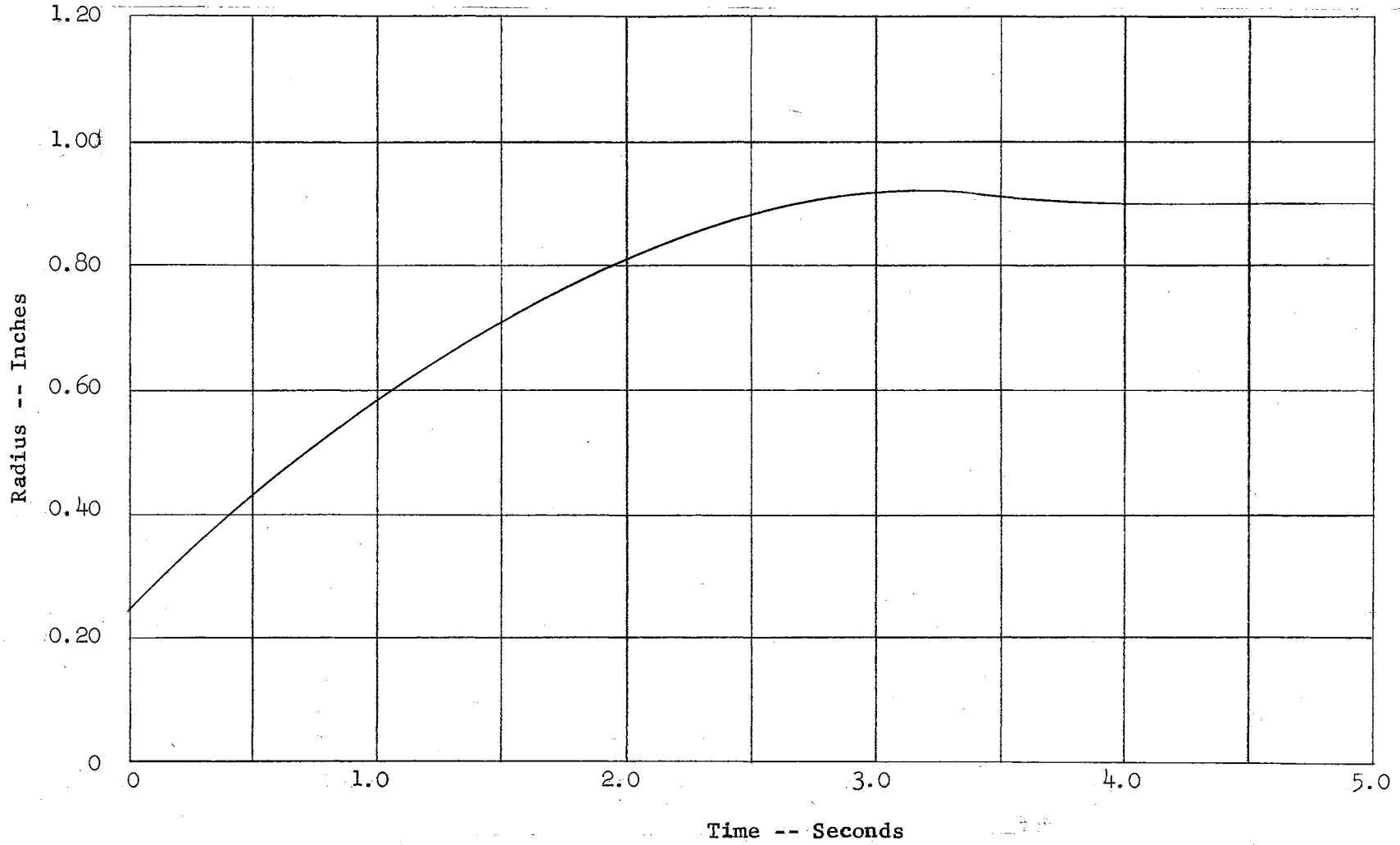

Figure 15. Separation Plot (Type II Glass Beads)

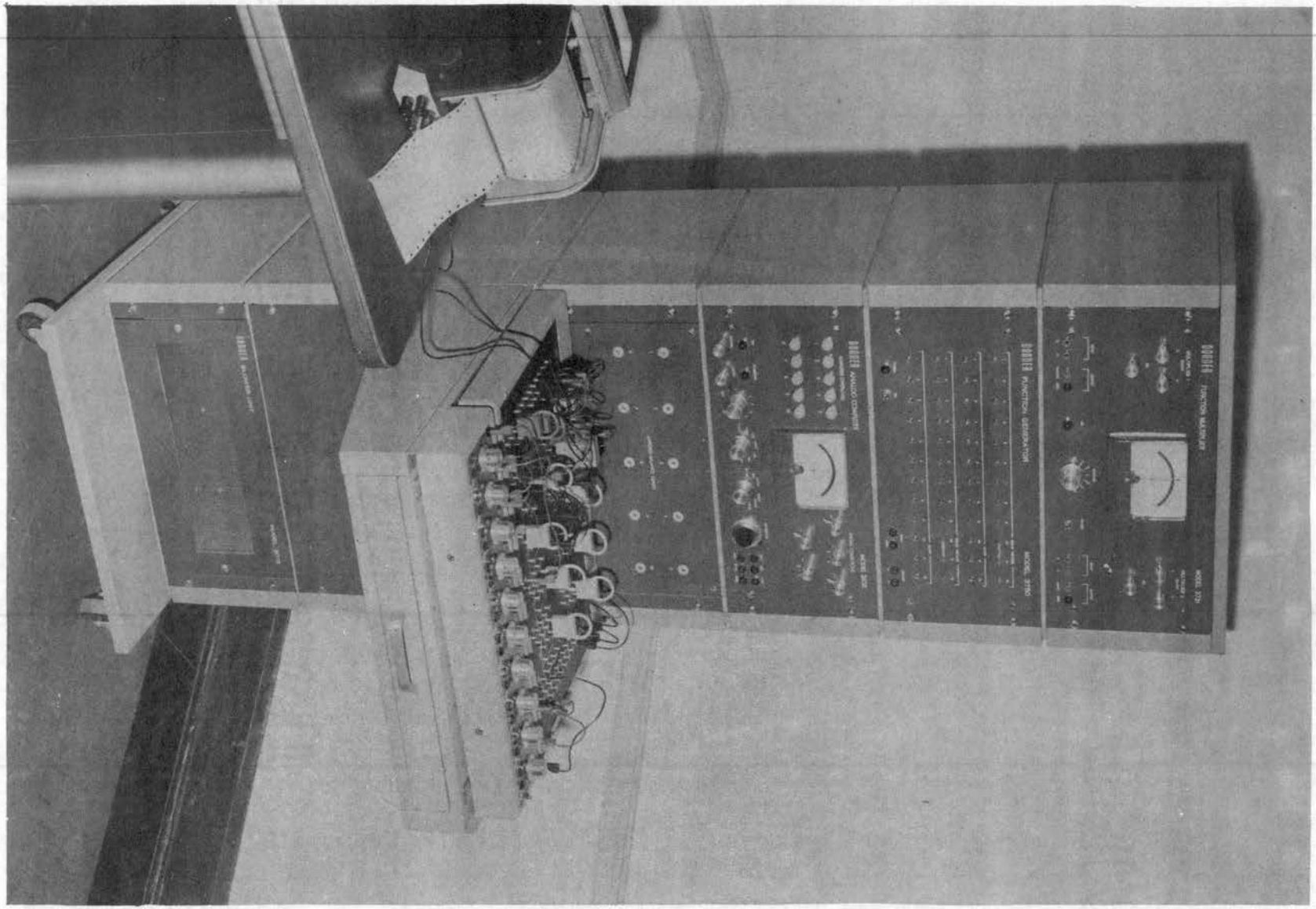

Figure 16. Electrical Analog Computer and Recorder

CHAPTER VI

EXPERIMENTAL VERIFICATION

This experimental investigation presents the relative separation ability of the hydroclone and the maximum size particle passed by it using Type I and Type II glass beads. Results were determined by examining fluid samples which had passed through the hydroclone. These samples were examined under a microscope with a micrometer stage eye-piece, after the sample was filtered through Millipore filter paper.

The sampling technique involves taking fluid samples immediately downstream from the hydroclone as soon as the injection of contaminates is completed upstream from the hydroclone. Figure 17 shows the schematic of the testing circuit. A picture of the overall testing apparatus is shown in Figure 18.

The contaminants were injected into the flow stream using an injection cylinder which was driven by a charged accumulator through a throttling valve. Valves placed in the circuit prevented premature injection and provided an alternate flow path through the injection cylinder to flush the remaining contaminant particles from the cylinder.

Fluid samples were caught in clean 100-milliliter bottles that had been rinsed with petroleum ether. Each sample was then dumped into a Millipore filter bowl which had been washed with petroleum ether and then filtered through the Millipore paper by pulling a vacuum on the flask beneath the Millipore assembly with a vacuum pump. A plastic cover was

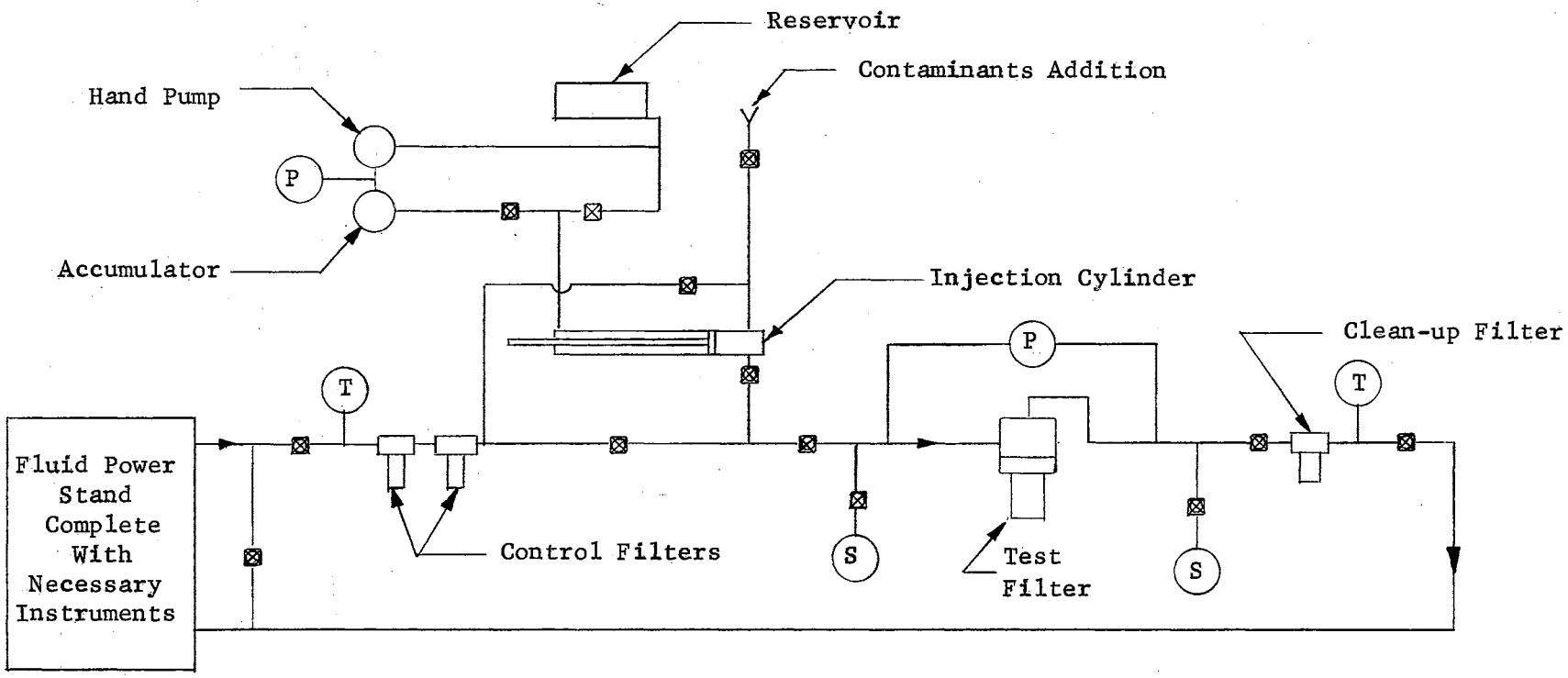

Figure 17. Test Circuit Schematic
T Temperature
S Sampling Connection

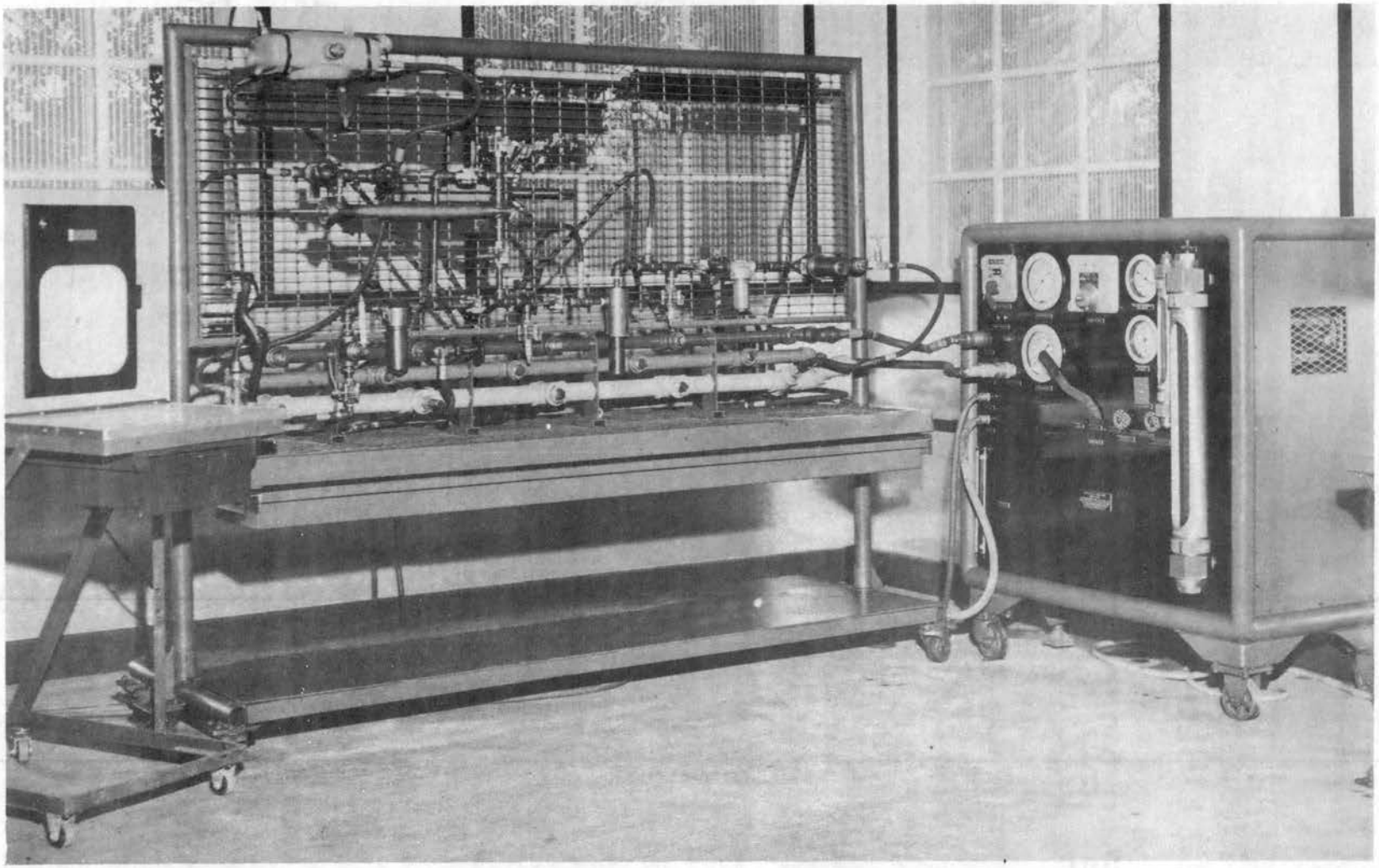

Figure 18. Test Circuit

placed over the Millipore equipment after the sample was dumped into the bowl. The same testing technique was used with both Type I and Type II glass beads.

The results of this test are found in Table IV. A clean sample indicates an estimate of only one or two glass beads per square on the filter paper. A dirty sample indicates five to ten times as many glass beads as found in a clean sample.

The maximum size particle found was 51 microns for Type I and 49 microns for Type II. This indicates that the hydroclone was functioning properly, because regardless of the size range of the beads involved the maximum particle passed is almost constant in size. A large number of glass beads were found in the underflow pot as further proof of its satisfactory performance. Fluid samples taken while using Type I glass beads were clean because the majority of the beads used were above the maximum size particle found. Consequently, the fluid samples taken while using Type II glass beads were dirty because the majority of the beads used were below the maximum size particle found.

TABLE IV

ANALYSIS OF FLUID SAMPLES

Flow Rate (gpm)	Filter Analysis	Minimum Diameter Bead (microns)
	Type I	
8	Clean	51
9	Clean	51
10	Clean	52
11	Clean	42
12	Clean	46
13	Clean	55
14	Clean	48
15	Clean	50
	Type II	
8	Dirty	49
9	Dirty	55
10	Dirty	58
11	Dirty	49
12	Dirty	40
13	Dirty	40
14	Dirty	44
15	Dirty	45

CHAPTER VII

SUMMARY AND CONCLUSIONS

The object of this investigation was to develop an analytical expression to evaluate the ability of a hydroclone to eliminate contaminants from hydraulic fluid. This study was conducted using a hydroclone built to functional design specifications. A constant flow rate of 8 gpm was used in the electrical analog application of the derived expression and in the experimental testing of the hydroclone. Comparison of the analytical and experimental results was made on the basis of the reaction of the hydroclone to Type I and Type II glass beads.

In this analysis the following basic assumptions were made:

1. The flow pattern predicted by Criner (2) is accurate.

2. Solids move through the hydroclone assuming the velocity of the fluid at every point except where motion relative to the fluid is induced by centrifugal forces.

3. A hydroclone will function without an air core in the inner spiral.

4. The radial acceleration can be considered as an important factor in particle movement.

5. Gravity and buoyant forces of a particle are small enough to be neglected.

The differential equation developed representing the radial movement of a particle in a viscous, incompressible medium in a hydroclone is as

follows:

$$\frac{D^2}{3}\rho_s\frac{dV_r}{dt}=\frac{D^2}{3}(\rho_s-\rho_l)\frac{V^2}{r}-6\mu V_r \quad . \tag{4-10}$$

Because an expression is needed for the tangential velocity, V, in terms of known quantities and no new variables, the following equation suggested and experimentally confirmed by Driessen (3) is used.

$$V=\frac{V_2 r_2}{r}\left[\frac{1+\ln\frac{r}{r_1}}{1+\ln\frac{r_2}{r_1}}\right] \quad . \tag{4-41}$$

Boundary conditions necessary in the derivation of equation (4-41) are $V = V_2$ when $r = r_2$ and $\frac{dv}{dr} = 0$ at $r = r_1$.

Using Type I glass beads during a flow of 8 gpm, equation (5-9) is formed.

$$\frac{d^2r}{dt^2}=f(r)-1.375\times10^{3}\frac{dr}{dt} \quad , \tag{5-9}$$

where

$$f(r)=\frac{4.56\times10^{4}}{r^3}(2.385+\ln r)^2 \quad . \tag{5-7}$$

After scaling equation (5-9) to the Donner Electrical Analog Computer and setting the initial conditions ($\frac{dr}{dt} = 0$ at $r = r_1$, where r_1 is the outer radius of the vortex finder) on the computer, a plot of radius, r, vs. time, t, was obtained as shown in Figures 14 and 15.

The effect of the flow pattern inside the hydroclone on both Type I and Type II glass beads can be easily correlated with the experimental study conducted. The larger particle (Type I) reached a radius of 1.00 in. in 1.375×10^{-3} sec which represents a radial velocity of 45.5 ft per

sec. The smaller particle (Type II) reached a radius of 0.92 in. in 3.125×10^{-3} sec which represents a radial velocity of 17.9 ft per sec. Thus the larger particle reaches a greater radius 2.54 times faster than a small particle.

The fact that a greater radius is reached quicker with a larger glass bead in planes near the bottom of the vortex finder and perpendicular to the axis helps prevent short-circuiting of the particles from the inlet nozzle directly to the overflow. Short-circuiting does not allow for the particles to separate from the feed stream because they leave at the vortex finder rather than follow the outer spiral to the "plane of no return" and thus to the underflow pot.

The experimental results verified the predicted separation ability of the hydroclone in regard to Type I and Type II glass beads. The maximum size particle is 51 micron for Type I and 49 microns for Type II. This indicates that the hydroclone was functioning properly, because regardless of the size range of the beads involved the maximum particle passed is almost constant in size. Five to ten times as many glass beads of Type II were found downstream of the hydroclone in comparison to the number of Type I glass beads found.

It can be concluded that equation (4-10), when applied to a small functional hydroclone, accurately predicts the ability of the hydroclone to eliminate contaminants from hydraulic fluid.

CHAPTER VIII

RECOMMENDATIONS FOR FUTURE STUDY

This investigation was of a hydroclone of fixed dimensions. These dimensions were assumed to provide adequate particle separation.

From previous investigations equation (2-1) represents a proven relationship between flow rate, pressure drop, inlet diameter, and overflow diameter. This relation could be combined with equation (4-10) such that the separation ability of a hydroclone can be evaluated in terms of hydroclone dimensions.

Experimental verification could be carried out by changing the overflow and inlet diameters for different flow rates. This would involve building interchangeable openings for the hydroclone.

The above approach is only one of many which could be taken in analyzing its performance. Future studies using different combinations of inlet, overflow, and underflow diameters programmed on the electrical analog computer could develop a hydroclone with greater contaminant separation ability.

A SELECTED BIBLIOGRAPHY

1. Dahlstrom, D. A, Ph.D. Thesis, Northwestern University (1949).

2. Criner, H. E., Paper presented at International Conference on Coal Preparation, Paris (1950).

3. Driessen, M. G., Rev. Ind. Minerale, page 449 (March 31, 1951).

4. Moder, J. J., Ph.D. Thesis, Northwestern University (1950).

5. Kelsall, D. F., Trans. Instn. Chem. Engrs., Vol. 30, page 87, (1952).

6. Kelsall, D. F., Chemical Engineering Science, Vol. 2, page 254, (1953).

7. Dahlstrom, D. A., Chemical Engineering Progress Symposium Series, Vol. 50, No. 15, page 41 (1954).

8. Haas, Nurmi, Whatley, and Engel, Chemical Engineering Progress, Vol. 50, No. 15, page 41 (1954).

9. Matschke and Dahlstrom, D. A., Chemical Engineering Progress, Vol. 34, No. 12, page 60, (December 1958).

10. Goldstein, S., Modern Developments in Fluid Dynamics, Vol. I, Oxford: Clarendon Press, page 104, 1938.

11. Binder, R. C., Fluid Mechanics, New York: Prentice-Hall Press, third edition, pages 171 and 179, 1955.

APPENDIX A

Nomenclature

F_a	Acceleration force, lb
F_c	Centrifugal force, lb
F_d	Drag force, lb
d_h	Diameter of hydroclone, in.
d_i	Inlet nozzle diameter of hydroclone, in.
d_o	Overflow nozzle diameter of hydroclone, in.
P	Pressure, psi
t	Time, sec
L	Length of hydroclone, in.
D	Diameter of particle, micron
D_{50}	Diameter of particle at 50% point, micron
Z	Axial coordinate or length, in.
r	Radius, in.
r_e	Equilibrium radius, in.
V	Tangential velocity, in. per sec
V_r	Radial velocity, in. per sec
V_z	Axial velocity, in. per sec
Q	Total flow rate, cu in. per sec
Q_u	Underflow flow rate, cu in. per sec
K	proportionality constant in equation (2-1)
K_1	Proportionality constant in equation (2-2)

C	Integration constant in equation (2-5)
C_1	Integration constant in equation (2-5)
K_2	Proportionality constant in equation (4-1)
K_3	Proportionality constant in equation (4-22)
A	Cross sectional flow area of unit height, sq in. per sec
C_3	Integration constant in equation (4-28)
C_4	Integration constant in equation (4-33)
A_i	Inlet nozzle area, sq in.
C_a	Capacitor, mfd
R_e	Resistor, megohm
E_i	Electrical potential in, volts
E_o	Electrical potential out, volts
P_o	Potentiometer reading, dimensionless

Greek Letters

π	Pi
Δ	Delta
μ	Mu, absolute viscosity, lb force per sq in.
ρ_l	Rho, mass density of liquid, lb mass per cu in.
ρ_s	Rho, mass density of solid, lb mass per cu in.
ν	Nu, kinematic viscosity, centistokes
ω	Omega, angular speed, radians per sec
ϕ	Phi, cylindrical polar coordinate in plane where Z is constant
β	Beta, coefficient of turbulent viscosity
α	Alpha, scale factor

Abbreviations

lb	Pounds
cu	Cubic
psi	Pounds per square inch
sq	Square
ft	Feet
sec	Seconds
in.	Inch, inches
gpm	Gallons per minute
mfd	Microfarad

Symbols

%	Per cent
∇	An operator

APPENDIX B

Apparatus and Equipment

1. Filtration Apparatus: Proposed Aeronautical Recommended Practice-598 issued by Society of Automotive Engineers, Inc.

2. Pressure Gage: Manufacturer, Barton Instrument Corp.; differential pressure range 0 to 300 psi, static pressure range 0 to 2000 psi.

3. Hydraulic Power Unit: Model X-003 designed and built under the Honor's Fellowship Program.

4. Precision Balance: Manufacturer, Christian Becker.

5. Glass Beads: Manufacturer, Minnesota Mining and Manufacturing Co.

6. Contamination Injection Circuit: Discussed in Fluid Contamination Project Report No. 2 for Contract No. AF 34(601)-5470 with Oklahoma City Air Materiel Area.

7. Electrical Analog Computer: Manufacturer, Donner Scientific Company; Model 3400.

8. Electrical Analog Variable Base Function Generator: Manufacturer, Donner Scientific Company; Model 3750.

9. Single Pen Recorder: Manufacturer, Texas Instruments; Model Recti/Riter.

VITA

Joel Sterling Gilbert

Candidate for the Degree of

Master of Science

Thesis: AN EVALUATION OF A SMALL HYDROCLONE USING ELECTRICAL ANALOG TECHNIQUES

Major Field: Mechanical Engineering

Biographical:

Personal Data: Born in Wichita, Kansas, August 29, 1935, the son of James S. and Mary G. Gilbert.

Education: Attended grade school in Billings, Oklahoma; graduated from Tonkawa High School, Oklahoma in 1953; received the Bachelor of Science degree from University of Oklahoma, Norman, Oklahoma, with a major in Mechanical Engineering, in January, 1958; completed the requirements for the Master of Science degree in August, 1960.

Experience: Employed by River Construction Company from June-September, 1955, as a surveyor's helper; employed by Continental Oil Company from June-September, 1956, as a maintenance inspector; employed by Kaiser Aluminum Company from June-September, 1957, as a technician; employed by Texas Instruments, Inc. from January 1958-January 1959, as an associate engineer; employed by Oklahoma State University from January 1959-August 1960, as a graduate assistant.

Honors and Awards: Received a four-year scholarship from Continental Oil Company; graduated from University of Oklahoma with "special distinction"; membership in Tau Beta Pi, Pi Tau Sigma and Sigma Tau engineering honoraries.

Professional Organizations: Member of the American Society of Mechanical Engineers.